Molecular Therapy
Original Article

Combination of Asiatic Acid and Naringenin Modulates NK Cell Anti-cancer Immunity by Rebalancing Smad3/Smad7 Signaling

Guang-Yu Lian,[1,3] Qing-Ming Wang,[1,3] Patrick Ming-Kuen Tang,[2] Shuang Zhou,[1] Xiao-Ru Huang,[1] and Hui-Yao Lan[1]

[1]Department of Medicine & Therapeutics and Li Ka Shing Institute of Health Sciences, The Chinese University of Hong Kong, Hong Kong SAR, China; [2]Department of Anatomical and Cellular Pathology, The Chinese University of Hong Kong, Hong Kong SAR, China

Transforming growth factor β1 (TGF-β1) plays a promoting role in tumor growth via a mechanism associated with hyperactive Smad3 and suppressed Smad7 signaling in the tumor microenvironment. We report that retrieving the balance between Smad3 and Smad7 signaling with asiatic acid (AA, a Smad7 inducer) and naringenin (NG, a Smad3 inhibitor) effectively inhibited tumor progression in mouse models of invasive melanoma (B16F10) and lung carcinoma (LLC) by promoting natural killer (NK) cell development and cytotoxicity against cancer. Mechanistically, we found that Smad3 physically bound Id2 and IRF2 to suppress NK cell production and NK cell-mediated cytotoxicity against cancer. Treatment with AA and NG greatly inhibited Smad3 translation and phosphorylation while it restored Smad7 expression, and, therefore, it largely promoted NK cell differentiation, maturation, and cytotoxicity against cancer via Id2/IRF2-associated mechanisms. In contrast, silencing Id2 or IRF2 blunted the protective effects of AA and NG on NK cell-dependent anti-cancer activities. Thus, treatment with AA and NG produced an additive effect on inactivating TGF-β1/Smad3 signaling, and, therefore, it suppressed melanoma and lung carcinoma growth by promoting NK cell immunity against cancer via a mechanism associated with Id2 and IRF2.

INTRODUCTION

Due to the genetic heterogeneity of cancer and the lesser specificity of cytotoxic drugs against cancer cells, immunotherapy by targeting the tumor microenvironment, rather than targeting tumor cells, may be a promising approach for anti-cancer therapy.[1] Among the signaling molecules in the tumor microenvironment, transforming growth factor β1 (TGF-β1) signaling has been proven to be a promoter in tumor growth, invasion, metastasis, and immunosuppression.[2–5] Therefore, altering from a supportive to inhibitory tumor microenvironment by targeting TGF-β1 signaling may represent a prospective therapeutic target.

As a vital transcription factor in TGF-β1 downstream signaling, Smad3 is essential for tumor progression.[6] Previous studies have confirmed that TGF-β1 promotes melanoma progression and immunosuppression via Smad3-dependent pathways,[7] while mice lacking Smad3 are resistant to chemical-induced skin carcinogenesis.[8,9] Our recent study also revealed that TGF-β1/Smad3 signaling is essential for cancer growth and invasion via a mechanism associated with suppressing natural killer (NK) cell immunity against cancer in the tumor microenvironment.[10] On the contrary, as an inhibitory Smad protein, Smad7 inhibits the phosphorylation of Smad2 and Smad3 via mechanisms associated with Smurfs-dependent ALK5 degradation, phosphatase GADD34-PP1c-mediated dephosphorylation of ALK5, and competitive inhibition of Smad3 interaction with ALK5.[11–13] A low expression level of Smad7 has been reported to correlate with poor prognosis and lymph node metastasis in pancreatic cancer.[14] Meanwhile, overexpression of Smad7 inhibits tumor growth in several cancer models, including hepatocellular carcinoma, melanoma, and lung metastasis in osteosarcoma.[15–18] A high expression of TGF-β1 is reported in many types of cancer, including melanomas and lung carcinoma.[19] Accordingly, we hypothesized that retrieving the balancing between Smad3 and Smad7 in a TGF-β1-rich tumor microenvironment may be a novel therapeutic strategy for TGF-β1-induced cancer progression.

Except for the direct effects on tumor growth and metastasis, TGF-β1 also acts as a potent immunosuppressor in the tumor microenvironment, which enables tumor evasion of immunosurveillance.[5,20] As a type of effector cells critical for innate immunity against cancer, NK cells rapidly respond to tumor formation and inhibit tumor progression independently from antigen presentation and T cell immunity.[21–23] However, NK cell-mediated cytotoxicity on tumor cells is blunted by TGF-β1 in the tumor microenvironment.[24–26] TGF-β1 is responsible for NK cell immaturity during mouse infancy through inhibiting the expression of E4BP4, T-bet, and GATA-3, which are

Received 13 February 2018; accepted 16 June 2018;
https://doi.org/10.1016/j.ymthe.2018.06.016.

[3]These authors contributed equally to this work.

Correspondence: Hui-Yao Lan, Department of Medicine & Therapeutics and Li Ka Shing Institute of Health Sciences, The Chinese University of Hong Kong, Hong Kong SAR, China.
E-mail: hylan@cuhk.edu.hk

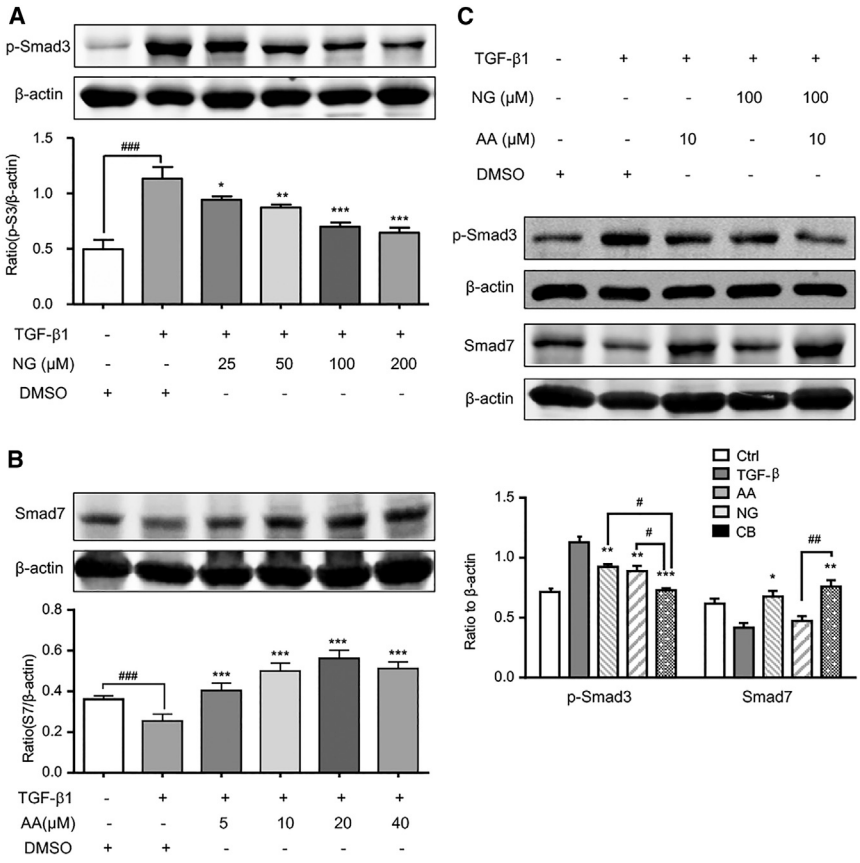

Figure 1. A Combination of AA and NG Rebalances Smad3 and Smad7 Signaling in Bone Marrow-Derived NK Cells *In Vitro*

(A) Pre-incubation of NG attenuates 15-min stimulation of TGF-β1 (5 ng/mL)-induced phosphorylation of Smad3 on bone marrow-derived NK cells in a dose-dependent manner. (B) Pre-incubation of AA restores Smad7 expression on bone marrow-derived NK cells in a dose-dependent manner with TGF-β1 (5 ng/mL) stimulation for 24 hr. (C) Western blot analysis shows the capability of AA (10 μM) and NG (100 μM) treatment on inhibiting Smad3 signaling while enhancing Smad7 signaling under a 5 ng/mL TGF-β1 condition on bone marrow-derived NK cells. Each bar represents the mean ± SEM for groups of three independent experiments; *$p < 0.05$, **$p < 0.01$, and ***$p < 0.001$ compared to TGF-β1; #$p < 0.05$, ##$p < 0.01$, and ###$p < 0.001$ as indicated.

crucial transcription factors for NK cell differentiation and terminal maturation.[10,27] Furthermore, TGF-β1 can markedly impair the NK cell-mediated cytotoxicity by suppressing granzymes and interferon (IFN)-γ productions and inhibiting NK cell activation.[24,28–31] As overactive Smad3 and/or loss of Smad7 are responsible for TGF-β1-induced immunosuppression of NK cells,[31] we postulated that re-balancing Smad3/Smad7 signaling may restore NK cell-mediated anti-tumor immunity in a TGF-β1-rich tumor microenvironment.

Asiatic acid (AA), a triterpene from *Centella asiatica*, functions as a Smad7 inducer, which is capable of inducing Smad7 in a dose-dependent manner to alleviate TGF-β1-induced liver fibrosis.[32] Naringenin (NG), a natural predominant flavanone isolated from citrus, functions as an effective inhibitor of Smad3 in liver and pulmonary fibrosis.[33,34] As a holistic approach, the principle of Traditional Chinese Medicine is to regain the balance and maintain the homeostasis of our body through the interactions within herbs or natural products. Our previous study identified that the combination of AA and NG can effectively alleviate TGF-β/Smad3-mediated renal fibrosis in the unilateral ureteral obstruction (UUO) model.[35] In the present study, we hypothesized that retrieving the balance between Smad3 and Smad7 signaling with AA and NG may enhance NK cell-mediated innate immune response against cancer in the tumor microenvironment.

RESULTS

AA and NG Effectively Restore the Balance of Smad3/Smad7 Signaling in NK Cells in a TGF-β1 Environment *In Vitro*

We first examined the efficacy of AA and NG on retrieving the balance of Smad3/Smad7 signaling in response to TGF-β1 in bone marrow-derived NK cells. As shown in Figures 1A and 1B, 5 ng/mL TGF-β1 enhanced the level of phosphorylated Smad3 at 15 min but suppressed Smad7 level at 24 hr, which was attenuated by pre-treatment with an optimal dosage of 100 μM NG or 10 μM AA. These inhibitory effects were further enhanced by treating NK cells with the combination of 10 μM AA and 100 μM NG (Figure 1C). Moreover, the combined treatment with AA and NG also produced an additive effect on inhibiting the phosphorylation of TβRI (p-ALK5) and expression of Smad3 under a TGF-β1 environment (Figure S1). Thus, the combination of AA and NG effectively rebalanced the TGF-β1/Smad signaling in NK cells.

The Combination of AA and NG Additively Inhibits Melanoma and Lung Carcinoma Growth in Syngeneic Mouse Models

We next determined the effective dosages of AA or NG on inhibiting B16F10 melanoma growth in a mouse model. As shown in Figures 2A–2D, treatment with either 10 mg/kg AA or 50 mg/kg NG effectively inhibited melanoma progression, although no further significant improvement in tumor growth was found with higher dosages of AA or NG. Therefore, AA at 10 mg/kg and NG at 50 mg/kg were selected as optimal dosages for evaluating the anti-tumor effect of rebalancing TGF-β1/Smad signaling on syngeneic mouse tumor models in the present study. Results shown in Figures 2E and 2F clearly demonstrated that the combined treatment with AA and NG additively restrained melanoma volume since day 10 after tumor inoculation when compared with the monotherapy of AA or NG. The anti-tumor efficacy of combination therapy was further validated

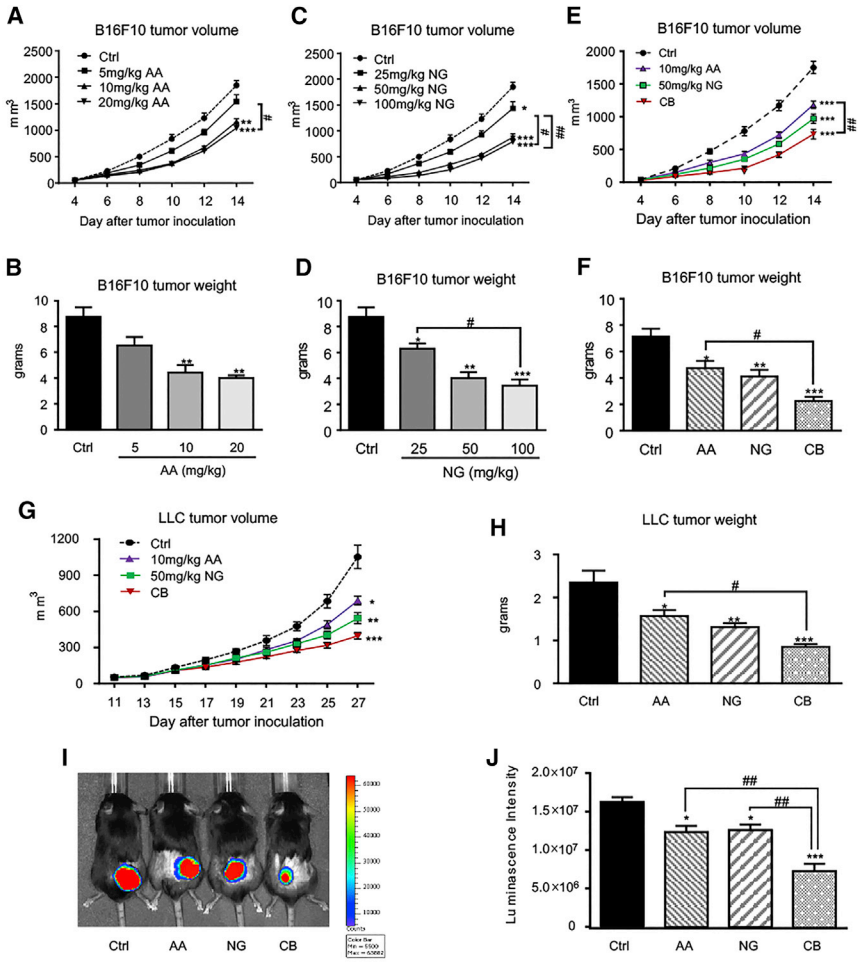

Figure 2. A Combination of AA and NG Produces a Better Inhibitory Effect on Tumor Growth Compared to Monotherapy

(A–D) Dose-dependent inhibitory effect of AA (A and B) or NG (C and D) on B16F10 melanoma volume and weight. (E and F) A combination therapy with an optimal AA (10 mg/kg/day) and NG (50 mg/kg/day) produces a better inhibitory effect on B16F10 melanoma growth compared to monotherapy as measured by tumor volume (E) and tumor weight (F). (G–J) Combination therapy with an optimal AA (10 mg/kg/day) and NG (50 mg/kg/day) produces a better inhibitory effect on LLC lung carcinoma compared to monotherapy, as determined by tumor volume (G), tumor weight (H), and bioluminescence imaging (I and J). Each bar represents the mean ± SEM for groups of six to eight mice; $^{*}p < 0.05$, $^{**}p < 0.01$, and $^{***}p < 0.001$ compared to control; #p < 0.05 and ##p < 0.01 as indicated.

with the Lewis lung cancer (LLC) mouse model, where a better antitumor effect on tumor growth, as determined by live bioluminescence reporter activities, tumor volumes, and tumor weights, over the monotherapy was achieved (Figures 2G–2J).

We also examined the potential side effects of AA and NG *in vivo*, and we found that treatment with AA (10 mg/kg), NG (50 mg/kg), and their combination neither alters the white blood cell counts nor causes toxicity to the kidney, heart, and liver of LLC-bearing mice, as serum levels of creatinine, lactate dehydrogenase (LDH), aspartate transaminase (AST), and alanine aminotransaminase (ALT) were not altered (Figure S2).

Rebalancing TGF-β1/Smad Signaling with AA and NG Enhances NK Cell Immune Response in a Tumor Microenvironment

We recently found that the number of tumor-infiltrating NK cells markedly decreased in the TGF-β1-rich tumor microenvironment of the LLC mouse model.[10] We thus examined whether restoring the balance of TGF-β1/Smad signaling with AA and NG promoted NK cell immune response in tumor microenvironments. As shown in Figure 3A, treatment with AA or NG increased the accumulation of tumor-infiltrating cytotoxic NK cells labeled with NK1.1 and NKp46, which was further enhanced in those receiving the combination treatment with AA and NG. Similarly, the combination of AA and NG also significantly promoted systemic NK cell response in peripheral blood, as determined by two-color flow cytometry (Figure 3B).

We then examined the potential mechanisms of AA and NG treatment on promoting tumor-infiltrating NK cells. As shown in Figures S3 and S4, AA and NG therapy did not influence the proliferative activity, apoptosis, and expression of CXCR3, a prerequisite for mouse NK cell infiltration.[36] These findings indicated that the therapeutic effects of AA and NG on tumor growth might be associated with promoting NK cell production in tumor-bearing mice. Furthermore, we also found that treatment with AA or NG not only increased the number of tumor-infiltrating $CD4^+$ and $CD8^+$ T cells but also decreased the number of $CD4^+Foxp3^+$ regulatory T cells without affecting $CD68^+$ macrophages (Figures S5 and S6). Nonetheless, treatment with AA, NG, or their combination did not influence serum levels of TGF-β1 in LLC-bearing mice (Figure S7) or major histocompatibility complex (MHC)-I expression on B16F10 and LLC cells (Figure S8).

It is well established that TGF-β1 impairs NK cell-mediated cytotoxicity via inhibiting the productions of various cytotoxic effectors, including IFN-γ, granzyme B (GB), and perforin.[24] We thus examined if treatment with AA or/and NG has an impact on NK cell cytotoxicity. As shown in Figures 4A and 4B, monotherapy with either AA or NG increased GB-secreting NK cells ($GB^+NK1.1^+$ cells) and IFN-γ-producing NK cells ($IFN\text{-}\gamma^+NK1.1^+$ cells) in the tumor microenvironment, which were further enhanced in LLC tumor-bearing mice that were treated with combined AA and NG. ELISA also detected a marked increase in IFN-γ and GB productions in the tumor

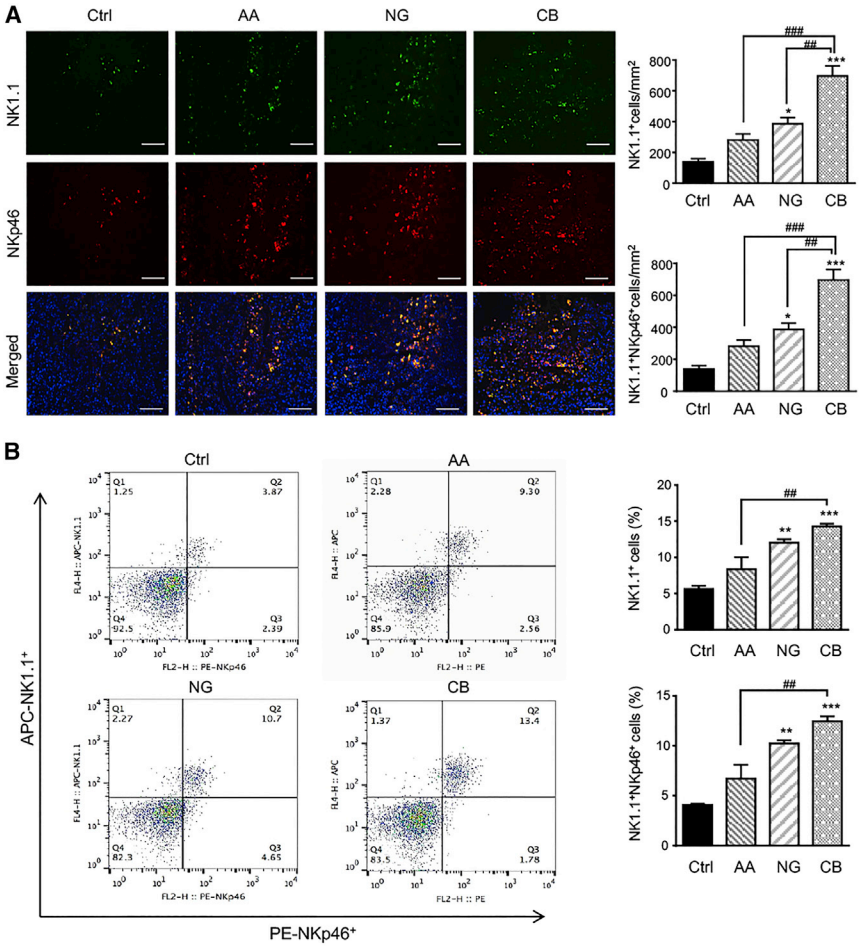

Figure 3. A Combination of AA and NG Largely Enhances Cytotoxic NK Cells Infiltrating the LLC Tumor Microenvironment

(A) Two-color immunofluorescence shows that numbers of cytotoxic NK cells (NK1.1$^+$NKp46$^+$ cells) in the LLC tumor microenvironment are largely increased in mice with the combination of AA and NG when compared to individual treatment. NK1.1, green; NKp46, red; DAPI, blue. (B) Two-color flow cytometry detects that numbers of cytotoxic NK cells (NK1.1$^+$NKp46$^+$ cells) in peripheral blood of LLC tumor-bearing mice are largely increased in mice with the combination of AA and NG when compared to individual treatment. Each bar represents the mean ± SEM for groups of three mice; *p < 0.05, **p < 0.01, and ***p < 0.001 compared to control; ##p < 0.01 and ###p < 0.001 as indicated. Scale bars, 100 μm.

tissue of mice treated with AA and NG when compared with those treated with control solvent or monotherapy (Figures 4C and 4D). This observation was further verified on cultured splenic NK cells treated with AA or NG, or combination therapy under TGF-β1 conditions (Figures 4E and 4F). Apart from promoting IFN-γ and GB productions by NK cells, combined treatment with AA and NG also resulted in severe tumor tissue necrosis in B16F10-bearing mice (Figure S9A), and it significantly attenuated TGF-β1-induced suppression of perforin, Fas ligand, and NKp46 expression but slightly elevated NKG2D expression in splenic NK cells (Figures S9B–S9E). However, expression of NKG2A by splenic NK cells was not altered by treatment with TGF-β1 or AA and NG (Figure S9F).

To examine whether rebalancing Smad3/Smad7 signaling with AA and NG can enhance the tumor-killing capacity of NK cells, we co-cultured AA- and NG-pretreated splenic NK cells with LLC cells at ratios of 5:1, 10:1, and 20:1 under 5 ng/mL TGF-β1 conditions. Results shown in Figure 4G clearly demonstrated that treatment with AA or NG increased NK cell-mediated cytotoxicity against LLC cells in a dose-dependent manner, which was further enhanced by the combination of AA and NG.

This *in vitro* observation was further supported in tumor tissues treated with AA and/or NG. As shown in Figure 5, combination treatment with AA and NG greatly blocked phosphorylation of Smad3 (p-Smad3) while it largely upregulated Smad7 expression in tumor-infiltrated NK cells when compared with the monotherapy in LLC-bearing mice.

Rebalancing TGF-β1/Smad Signaling with AA and NG Promotes NK Cell Production via Id2 and IRF2-Associated Mechanisms

We then examined the potential mechanisms by which treatment with AA and NG promotes NK cell response *in vitro*. As shown in Figure 6A, the addition of TGF-β1 significantly suppressed NK cell production in a dose-dependent manner. Numerically, TGF-β1 at a dose of 5 ng/mL largely reduced NK1.1$^+$CD122$^+$ cell (immature NK cell) proportion from 80% to 11%. Treatment with AA or NG partially reversed the inhibitory effect of TGF-β1 on NK1.1$^+$CD122$^+$ cells, which was largely increased by the combined treatment with AA and NG (Figure 6B).

It is known that NK cell differentiation and maturation are strictly regulated by various transcription factors, including Id2 and IRF2.[37,38] We then examined whether enhancing NK cell maturation by AA and NG is transcriptionally regulated by Id2 and IRF2. Real-time PCR detected that, compared to control or monotherapy with AA or NG, the combination of AA and NG largely enhanced the expression of Id2 and IRF2 in peripheral blood NK cells of LLC tumor-bearing mice (Figures 7A and 7B). This *in vivo* observation was further confirmed *in vitro* with bone marrow-derived NK cells: TGF-β1-induced suppression of Id2 and IRF2 in NK cells was attenuated by monotherapy with AA or NG, and it was further blunted by AA and NG combination therapy (Figures 7C–7E). Therefore, rebalancing Smad3/Smad7 signaling with AA and NG treatment may enhance NK cell maturation in

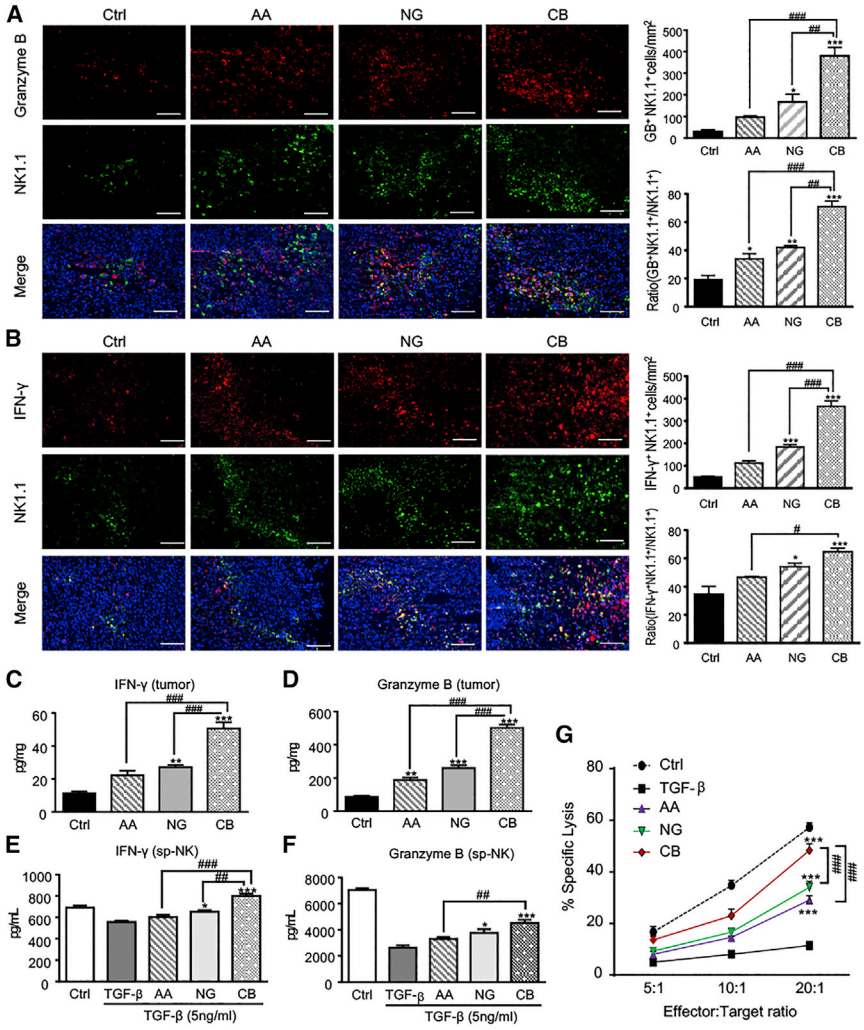

Figure 4. Rebalancing Smad3/Smad7 Signaling with AA and NG Enhances the Production of IFN-γ and Granzyme B by NK Cells

(A and B) Two-color immunofluorescence detects NK1.1$^+$ granzyme B$^+$ (A) and NK1.1$^+$ IFN-γ$^+$ (B) NK cells infiltrating the LLC tumor microenvironment. NK1.1, green; IFN-γ or granzyme B, red; DAPI, blue. Each bar represents the mean ± SEM for groups of three to four mice. Scale bar, 100 μm. (C and D) ELISA shows IFN-γ (C) and granzyme B (D) levels in homogenized LLC tissue. *p < 0.05, **p < 0.01, and ***p < 0.001 compared to control; #p < 0.05, ##p < 0.01, and ###p < 0.001 as indicated. (E and F) Effect of AA (10 μM), NG (100 μM), and their combination on the productions of IFN-γ (E) and granzyme B (F) in splenic NK cells (sp-NK) with TGF-β1 (5 ng/mL) stimulation detected by ELISA. (G) NK cell cytotoxicity assay with AA or/and NG pre-treated bone marrow-derived NK cells as effector cells and LLC as target cells at E:T ratios of 5:1, 10:1, and 20:1 in the TGF-β1 (5 ng/mL) condition. Each bar represents the mean ± SEM for groups of three independent experiments; *p < 0.05 and ***p < 0.001 compared to TGF-β1; ##p < 0.01 and ###p < 0.001 as indicated.

the TGF-β1-rich tumor microenvironment through restoring the expression of Id2 and IRF2, two essential transcription factors respectively responsible for NK cell lineage commitment and NK cell terminal maturation.[39,40] As shown in Figures 8A and S10, silencing Id2 on NK cells significantly impaired the protective effect of AA and NG on the production of immature NK cells (NK1.1$^+$DX5$^-$ cells) and terminal mature NK cells (NK1.1$^+$ DX5$^+$CD11b$^+$ cells) under TGF-β1 conditions, whereas silencing IRF2 had no significant influence on immature NK cells (NK1.1$^+$ DX5$^-$ cells) in response to AA and NG treatment, but it inhibited terminal maturation of NK cells as demonstrated by reducing the proportion of NK1.1$^+$DX5$^+$CD11b$^+$ cells. This was consistent with a previous report that IRF2 is a checkpoint regulator during the process of NK cell terminal maturation.[40] Interestingly, knockdown of Id2 and IRF2 on mature NK cells was able to block AA- and NG-induced GB expression under TGF-β1 conditions, but it did not alter the expression of IFN-γ, perforin, and Fas ligand (Figure S11).

We next examined the regulatory mechanism of TGF-β1/Smad signaling in Id2/IRF2-dependent NK cell differentiation and maturation, and we found predicted Smad3-binding sites (SBSs) in the proximity of IRF2 3′ UTR and 5′ UTR and another two within Id2 3′ UTR with ECR browser (rVista 2.0, https://rvista.dcode.org/).[41] Chromatin immunoprecipitation (ChIP) assay confirmed that the addition of TGF-β1 markedly enhanced the physical binding of Smad3 protein on the genomic sequences of Id2 3′ UTR and IRF2 near 3′ UTR (Figures 8B and 8C), thereby suppressing the transcription of Id2 and IRF2 in NK cells. This finding demonstrated a direct transcriptional inhibitory mechanism of TGF-β1/Smad3 on Id2/IRF2-dependent NK cell development.

DISCUSSION

Accumulating evidence demonstrates that over-activation of Smad3 and reduction of Smad7 signaling play vital roles in a variety of TGF-β1-induced pathological conditions, including tissue fibrosis and tumor progression.[10,35] In the present study, we provided the first evidence for rebalancing the TGF-β1/Smad3/Smad7 signaling in a tumor microenvironment by a combination therapy with AA and NG to inhibit tumor progression in mouse models of melanoma and lung carcinoma. Mechanistically, we revealed that AA exerted as a Smad7 inducer to suppress Smad3 activation through an ALK5-dependent mechanism, whereas NG functioned as a Smad3 inhibitor to block Smad3 signaling translationally and post-translationally without altering Smad7 expression. Accordingly, retrieving the balance between Smad3 and Smad7 signaling may account for the

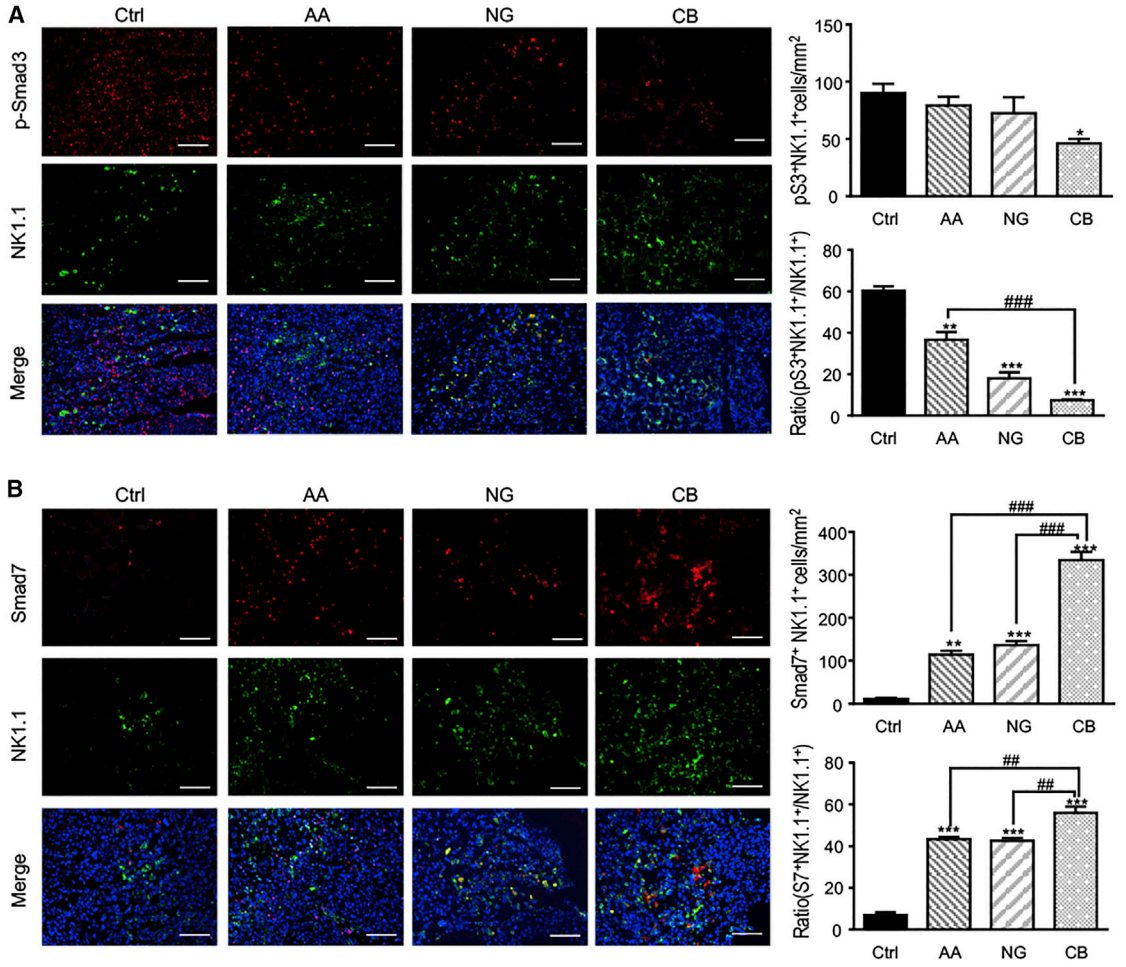

Figure 5. A Combination of AA and NG Effectively Rebalances TGF-β1/Smad Signaling in Tumor-Infiltrating NK Cells by Additively Repressing Smad3 Phosphorylation while Enhancing Smad7 Expression

(A and B) Two-color immunofluorescence detecting NK1.1$^+$p-Smad3$^+$ (A) and NK1.1$^+$Smad7$^+$ (B) NK cells in the LLC tumor microenvironment. NK1.1, green; p-Smad3 or Smad7, red; DAPI, blue. Each bar represents the mean ± SEM for groups of three to four mice; *p < 0.05, **p < 0.01, and ***p < 0.001 compared to control; ##p < 0.01 and ###p < 0.001 as indicated. Scale bar, 100 μm.

synergic effect of the combination of AA and NG therapy on suppressing B16F10 melanoma and LLC lung carcinoma progression.

Importantly, we identified that enhanced NK cell immunity may be a key mechanism through which AA and NG therapy suppressed B16F10 and LLC tumor progression. As an indispensable component in tumor immunosurveillance, NK cells exert a rapid innate immune response to tumorigenesis and cancer progression by directly triggering tumor cell death.[21,23] However, NK cell immune response has been severely suppressed by hyperactive TGF-β1/Smad signaling in a tumor microenvironment characterized by markedly decreased NK cell development and loss of cytotoxicity against cancer.[27,42] We previously found that the disruption of Smad3 or pharmacological inhibition of Smad3 protects against melanoma and lung carcinoma progression in mice by promoting NK cell immunity.[10] In the present study, we found that rebalancing TGF-β/Smad signaling by AA and NG was capable of restoring the NK cell immunity against cancer in the TGF-β1-abundant tumor microenvironment by largely increasing both NK cell number (NK1.1$^+$NKp46$^+$ cells) and anti-cancer activities, such as productions of IFN-γ, GB, perforin, FasL, and the expression of activation receptor NKp46.

Mechanistically, here we also identified that the inhibition of Smad3-mediated immunosuppression on Id2/IRF2-dependent NK cell development and function may be an important mechanism by which rebalancing Smad3/Smad7 signaling with AA and NG effectively inhibited melanoma and lung carcinoma progression. It is well established that NK cell development is strictly programmed by a number of transcription factors and TGF-β1 inhibits CD11b^{high} CD43^{high} NK cells via suppressing both T-bet and GATA3.[27] Our recent study also demonstrated that TGF-β1 via Smad3 promotes cancer progression by inhibiting E4BP4-mediated NK cell

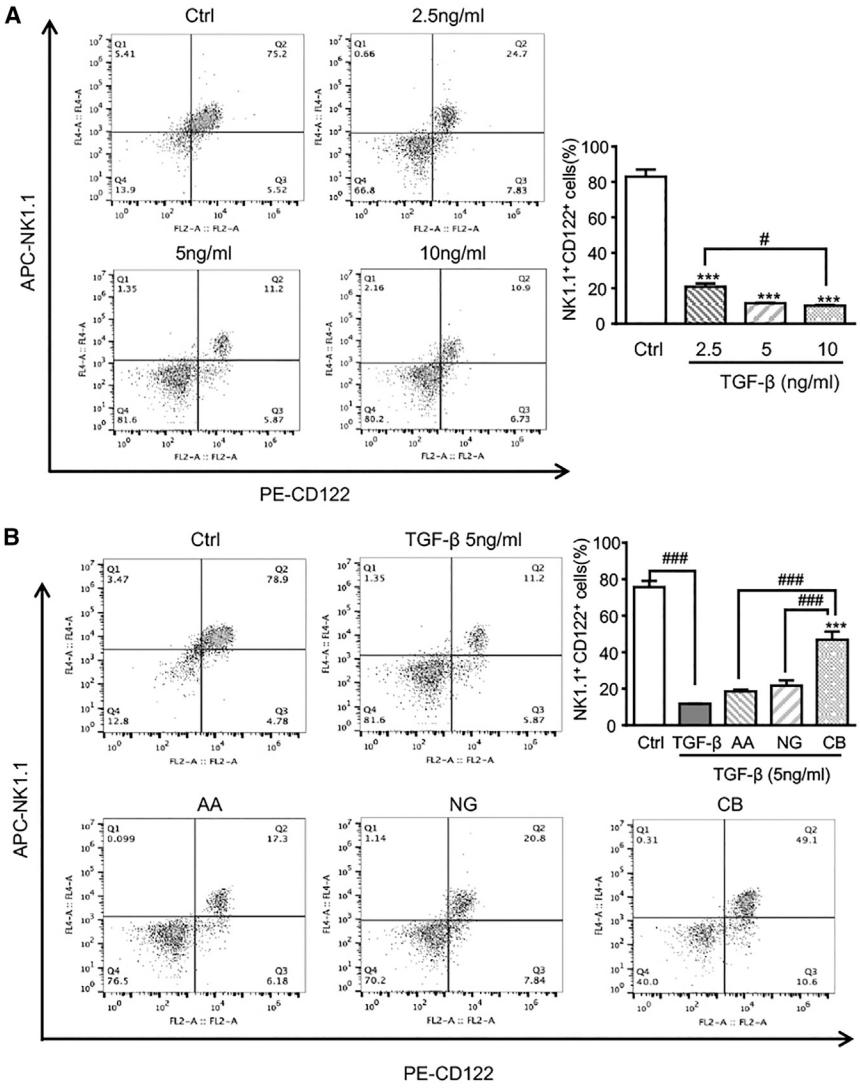

Figure 6. Retrieving the Balance of Smad3/Smad7 Signaling with AA and NG Attenuates TGF-β1-Induced Inhibition on NK Cell Differentiation

(A) Flow cytometry shows the inhibitory effect of TGF-β1 on NK cell differentiation as determined by $NK1.1^+$ $CD122^+$ population in bone marrow-derived NK cells (day 9). ***$p < 0.001$ compared to control; #$p < 0.05$ as indicated. (B) Flow cytometry detects the effects of AA, NG, and their combination on bone marrow-derived NK differentiation in response to TGF-β1 (5 ng/mL). Each bar represents the mean ± SEM for groups of three independent experiments; ***$p < 0.001$ compared to TGF-β1; ###$p < 0.001$ as indicated.

development.[10] In the present study, we further identified that the combined AA and NG treatment promoted Id2/IRF2-associated NK cell differentiation and maturation via rebalancing the TGF-β1/Smad signaling. Id2, as the antagonist of E proteins, is indispensable for the development of NK cell precursor to immature NK cells, and it is also involved in NK maturation;[39,43,44] meanwhile, IRF2 protects premature NK cells from apoptosis to ensure NK cells complete GATA3-induced terminal maturation as well as maintain NK cell proliferation.[40,45] Here we identified that Smad3 directly interacted with the 3′ UTR of Id2 and IRF2 to suppress their transcription. This may well explain the therapeutic effects of AA and NG on TGF-β1-induced suppression of Id2-dependent NK cell lineage commitment ($NK1.1^+CD122^+$ cells) and IRF2-dependent NK cell terminal maturation ($NK1.1^+DX5^+CD11b^+$ cells). Silencing Id2 or IRF2 respectively impaired the rescuing effect of AA and NG on the production of immature ($NK1.1^+DX5^-$) or mature ($NK1.1^+DX5^+CD11b^+$) NK cells in the TGF-β1-rich environment, further confirming the therapeutic mechanisms of AA and NG on NK cell differentiation. Taken together, these results suggested that rebalancing Smad3/Smad7 signaling with AA and NG increased NK cell production in tumor-bearing mice via alleviating the inhibition of TGF-β1 on Id2- and IRF2-dependent NK cell differentiation and maturation.

In addition to promoting NK cell production in the TGF-β1-rich tumor microenvironment, rebalancing Smad3/Smad7 signaling also strengthened NK cell-mediated cytotoxicity against tumor by elevating IFN-γ and GB productions. Massagué et al. identified that TGF-β1 activates Smad2/3 together with ATF1 transcription factors to directly bind to the promoter region of both IFNG and GZMB to induce a significant reduction in IFN-γ and GB productions.[46,47] Consistently, rebalancing Smad3 and Smad7 signaling with AA and NG debilitated the inhibition of TGF-β1 on IFN-γ and GB productions by NK cells and effectively elevated NK cell cytotoxicity against tumor cells, as noted in this study.

It should be pointed out that, as natural herb-derived compounds, AA and NG may not exert their anti-cancer effects thoroughly via the NK cell-dependent mechanism. It is well documented that TGF-β1 promotes cancer progression by altering T cell immunity in a tumor microenvironment.[48–50] In the present study, we also found the combined treatment with AA and NG increased both $CD4^+$ and $CD8^+$ T cells while suppressing $CD4^+Foxp3^+$ regulatory T cells, suggesting that enhanced T cell immunity against cancer may be another mechanism whereby combined AA and NG therapy additively suppressed cancer growth in mouse models of melanoma and lung carcinoma. In addition, AA may work via other mechanisms to inhibit cancer growth, such as inhibiting angiogenesis in glioma and inducing apoptosis and cell-cycle arrest of tumor cells.[51–54] The anti-cancer effect of NG is also associated with reducing regulatory T cells while

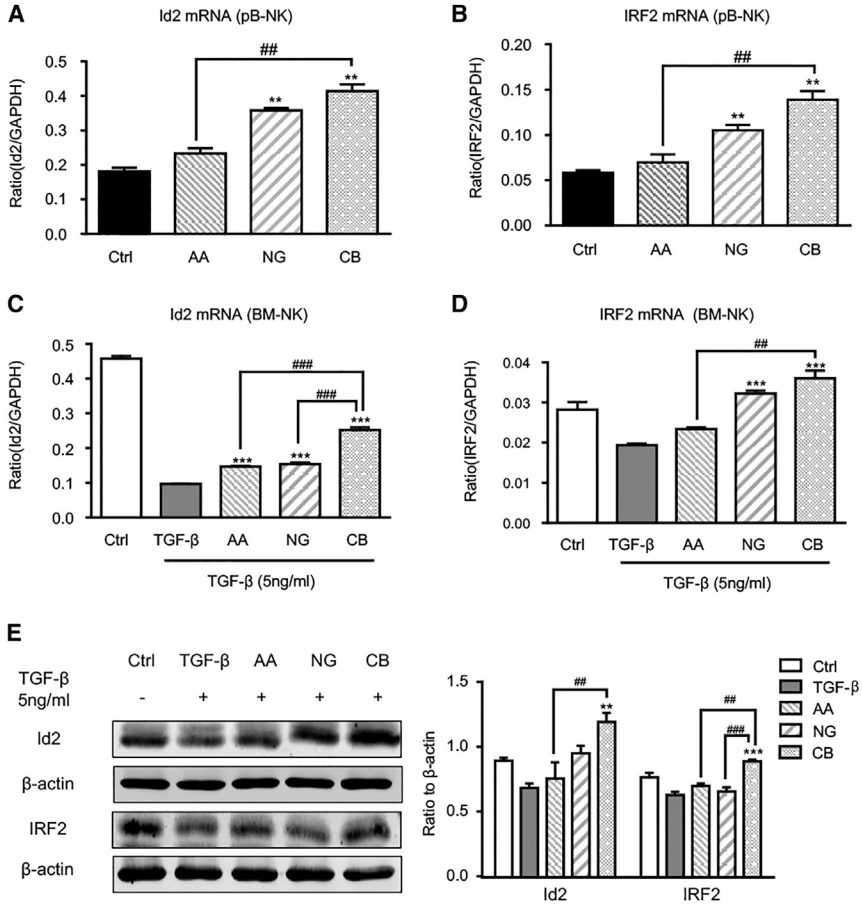

Figure 7. Rebalancing TGF-β1/Smad Signaling with AA and NG Reverses the Suppressive Effect of TGF-β1 on Id2 and IRF2 Expression

(A and B) mRNA levels of Id2 (A) and IRF2 (B) in peripheral blood NK cells (pB-NK) isolated from LLC-bearing mice detected by real-time PCR. **p < 0.01 compared to control; ##p < 0.01 as indicated. (C and D) mRNA levels of Id2 (C) and IRF2 (D) in AA and NG pre-treated bone marrow-derived NK cells (BM-NK) with TGF-β1 (5 ng/mL) stimulation detected by real-time PCR. (E) Id2 and IRF2 expression in AA and NG pre-treated bone marrow-derived NK cells with TGF-β1 (5 ng/mL) stimulation measured by western blot. Each bar represents the mean ± SEM for groups of three to four mice or groups of three independent experiments; **p < 0.01 and ***p < 0.001 compared to TGF-β1; ##p < 0.01 and ###p < 0.001 as indicated.

suppressing epithelial-mesenchymal transition (EMT)-dependent tumor metastasis and inhibiting tumor growth by TRAIL-induced apoptosis as well as inducing cell-cycle arrest.[34,55–57]

Notably, treatment with AA and NG was relatively safe. This is because the combined use of AA and NG rebalanced, rather than terminated, TGF-β/Smad signaling, and thus it did not cause severe side effects such as autoimmune diseases, as seen in TGF-β-deficient mice.[58,59] In addition, no detectable side effects were noted, including bone marrow suppression and toxicity to kidney, heart, and liver in tumor-bearing mice treated with AA and NG. However, the potential toxicity of AA and NG in human subjects remains unknown and requires further investigation.

In summary, the combined use of AA and NG produced an additive effect on suppressing experimental melanoma and lung carcinoma growth. Rebalancing Smad3/Smad7 signaling in a tumor microenvironment and thus promoting NK cell immunity against tumor by debilitating TGF-β1-mediated inhibition of Id2/IRF2-associated NK cell production and anti-tumor activities may be the mechanisms through which AA and NG effectively suppressed melanoma and lung carcinoma progression. Results from this study suggested that AA and NG may be promising immunotherapy for melanoma and lung carcinoma clinically.

MATERIALS AND METHODS

NK Cell Culture *In Vitro*

After euthanasia, bone marrow cells were isolated from C57BL/6 mice, and then they were seeded at the density of 1×10^6 cells/mL in MEMα medium (Gibco, Thermo Fisher Scientific, MA, USA), containing 10% fetal bovine serum (FBS) supplemented with 1 ng/mL interleukin-7 (IL-7), 10 ng/mL Flt3L, 30 ng/mL stem cell factor (SCF), 50 ng/mL IL-15 (PeproTech, NJ, USA), and 50 mM β-mercaptoethanol (Gibco, Thermo Fisher Scientific, MA, USA), and cultured for 4 days. Then we transferred cells to MEMα medium containing 10% FBS supplemented with 50 ng/mL IL-15, 20 ng/mL IL-2, and 50 mM β-mercaptoethanol to induce NK cell maturation for another 5 days.

To isolate splenic NK cells, spleen tissues were gently mashed through a 40-μm cell strainer into a 50-mm^2 dish, and then splenic NK cells were isolated with the NK Cell Isolation Kit II (Miltenyi Biotec, CA, USA). Splenic NK cells were cultured in MEMα medium containing 10% FBS supplemented with 50 ng/mL IL-15, 20 ng/mL IL-2, and 50 mM β-mercaptoethanol.

Western Blot

Tumor tissues and cultured NK cells were lysed with ice-cold radioimmunoprecipitation assay (RIPA) buffer; then subjected to western blot analysis with primary antibodies against Smad7, Id2, β-actin (Santa Cruz Biotechnology, CA, USA), p-Smad3, IRF2 (Cell Signaling Technology, MA, USA), p-ALK5 (Abcam, MA, USA), and Smad3 (Invitrogen, Thermo Fisher Scientific, MA, USA) overnight at 4°C; and subsequently incubated with IRDye 800-conjugated secondary antibody (Rockland Immunochemicals, PA, USA). Target protein

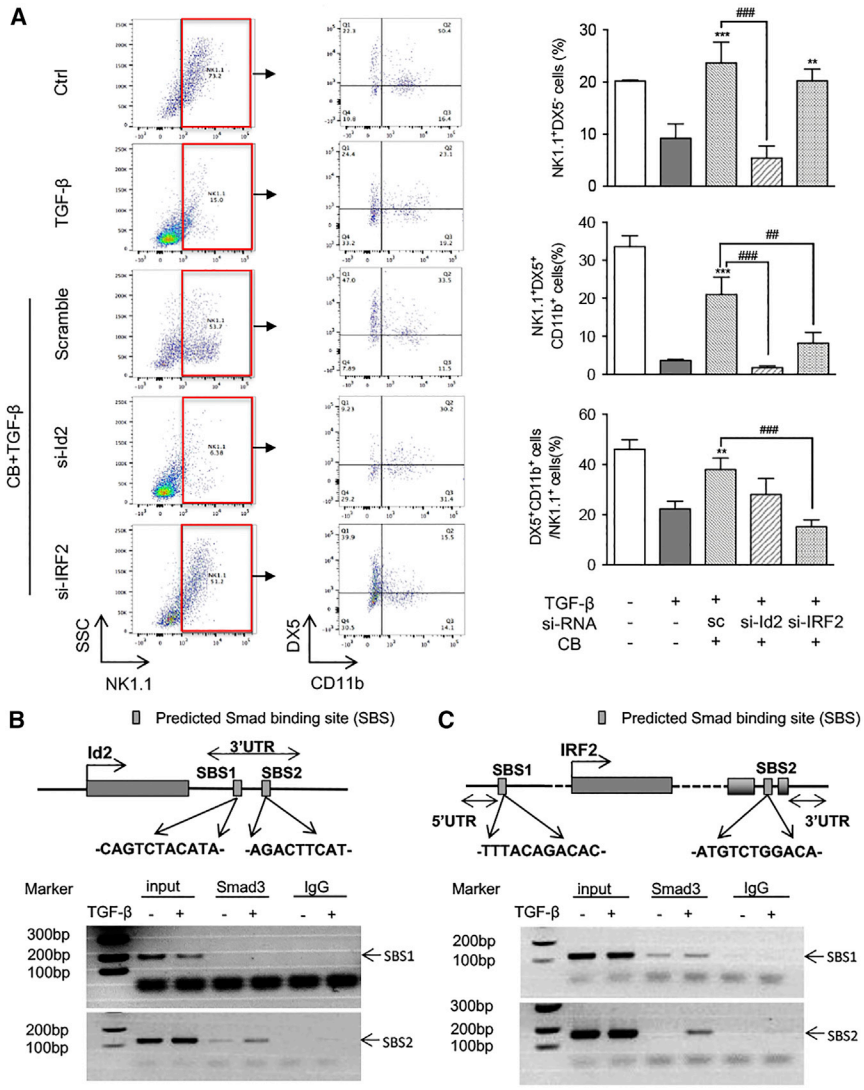

Figure 8. Smad3 Inhibits NK Differentiation and Maturation as a Transcriptional Repressor for Id2 and IRF2

(A) $NK1.1^+DX5^+CD11b^+$ cells detected by three-color flow cytometry. Bone marrow-derived NK cells were transfected with scramble sequence (sc), si-Id2, or si-IRF2; then cultured with AA (10 μM) and NG (100 μM) under TGF-β1 (5 ng/mL) conditions for 9 days; and collected for flow cytometry analysis. (B and C) ChIP assay shows that the addition of TGF-β1 (5 ng/mL) induces Smad3 directly binding to the predicted Smad-binding site on the 3′ UTR of both Id2 (B) and IRF2 (C) gene on bone marrow-derived NK cells. Each bar represents the mean ± SEM for three independent experiments; $^{**}p < 0.01$ and $^{***}p < 0.001$ compared to TGF-β1-treated group; $^{\#\#}p < 0.01$ and $^{\#\#\#}p < 0.001$ as indicated.

expression was detected by Li-Cor/Odyssey infrared image system (LI-COR Biosciences, NE, USA) and analyzed with ImageJ software (NIH, Bethesda, MD, USA).

Syngeneic Mouse Tumor Models and Treatments

B16F10 melanoma syngeneic tumor model was generated in C57BL/6 male mice (at 8 weeks of age and 25 g body weight) via subcutaneous injection of 1×10^6 B16F10 cells (CRL-6475, ATCC). The LLC syngeneic tumor model was also generated in C57BL/6 male mice via subcutaneous injection of 2×10^6 luciferase-labeled LLC cells (CRL-1642, ATCC). When average tumor size reached 50 mm^3, mice were randomly divided into four groups with six to eight in each group, respectively receiving drug administration as described below. Tumor progression was monitored by calculating tumor volume with vernier calipers as well as by bioluminescence imaging with IVIS Spectrum system (Xenogen, PerkinElmer, MA, USA). Changes in tumor pathology were determined by periodic acid Schiff (PAS) staining. All animal experiments were carried out by a protocol approved by the Animal Ethics Experimental Committee at the Chinese University of Hong Kong.

Two Traditional Chinese Medicine (TCM)-based drugs were used in this study, including AA (95% high performance liquid chromatography [HPLC] purified, Nanning, China) and NG (98% HPLC purified, Xian, China). Both drugs were dissolved in the mixture of DMSO and Tween-80 (at the ratio of 1:4) as a solvent, which was further diluted 20 times with saline as a working solution. Tumor-bearing mice were randomly divided into groups for various treatment with AA at a dose of 10 mg/kg body weight, NG at a dose of 50 mg/kg body weight, or combination therapy with AA (10 mg/kg) and NG (50 mg/kg) every day via intraperitoneal injection. Studies were carried out by a protocol approved by the Animal Ethics Experimental Committee at the Chinese University of Hong Kong.

Determination of Potential Side Effects in Mice

The number of white blood cells was counted with peripheral blood collected from LLC-bearing mice 27 days after tumor inoculation. Serum creatinine, AST, ALT, and LDH were measured with Creatinine LiquiColor Test, ALT/SGPT Liqui-UV Test, and AST/SGOT Liqui-UV Test from Stanbio Laboratory and QuantiChrom Lactate Dehydrogenase Kit (DLDH-100) from BioAssay.

Immunofluorescence Staining

Immunofluorescence staining was performed with 5 μm PLP-fixed frozen sections. Primary antibodies used for immunofluorescence staining included Alexa488-conjugated anti-mouse NK-1.1,

Alexa594-conjugated anti-mouse CD68 (BioLegend, CA, USA), phycoerythrin (PE)-conjugated anti-mouse NKp46, fluorescein isothiocyanate (FITC)-conjugated anti-mouse CD8a, FITC-conjugated anti-mouse CD4, PE-conjugated anti-mouse Foxp3 (eBioscience, CA, USA), anti-p-Smad2/3 (Santa Cruz Biotechnology, Santa Cruz, CA), anti-Smad7, anti-interferon gamma, and anti-GB (Abcam, MA, USA), followed by PE- or Alexa 594-conjugated anti-rabbit secondary antibodies. All slides were mounted with DAPI-containing mounting medium and then analyzed with a fluorescence microscope (Leica Microsystems, Wetzlar, Germany).

Flow Cytometry Analyses

Peripheral blood NK cells and cultured NK cells were harvested, blocked with rat anti-mouse CD16/CD32 antibody (BD Pharmingen, CA, USA), and then analyzed with various antibodies, including antigen-presenting cell (APC)-conjugated anti-mouse NK1.1, PE-conjugated anti-mouse NKp46, PE-conjugated anti-mouse CD122, PE-conjugated anti-mouse DX5 (eBioscience, CA, USA), and Alexa 488-conjugated anti-mouse/human CD11b antibody (BioLegend, CA, USA). After immunostaining, cells were resuspended with 500 μL PBS and analyzed with BD AccuriTM C6 Cytometer (BD Biosciences, CA, USA).

MTT Assay

Bone marrow-derived NK cells were seeded on a 96-well plate at the density of 1×10^4/well and treated with solvent (DMSO) and AA and NG individually or in combination for 44 hr. Methyl-thiazoldiphenyl tetrazolium (MTT, 5 mg/mL) was added to each well and incubated for another 4 hr at 37°C. Supernatant was removed and 100 μL DMSO was added to each well, then absorbance at 490 nm was measured using a plate reading spectrophotometer. All data were calculated as a ratio against control.

Detection of Apoptosis Using Annexin V/Propidium Iodide Staining

Bone marrow-derived NK cells pre-incubated with solvent (DMSO) and AA and NG individually or in combination for 24 hr were stimulated with 5 ng/mL TGF-β1 for another 24 hr. Cells were collected by centrifuging at 3,000 rpm for 5 min at 4°C, and then they were stained with Annexin-V-FLUOS Staining Kit (Sigma-Aldrich, MO, USA) and immediately analyzed using a flow cytometer.

RNA Extraction and Real-Time PCR

Total RNA was isolated from tumor tissue or cultured cells with PureLink RNA Mini Kit (Life Technologies, NY, USA). RNA concentration was measured with Spectrophotometers Nanodrop (ND-2000, Thermo Fisher Scientific, MA, USA). The real-time PCR program was performed with Bio-Rad iQ SYBR Green supermix with Opticon2 (Bio-Rad, Hercules, CA, USA) on CFX96 Touch Real-Time PCR Detection System (Bio-Rad, Hercules, CA, USA). GAPDH was used as the internal control, and the ratio of target to GAPDH was calculated as $\Delta Ct = Ct\ (target) - Ct\ (GAPDH)$, ratio (target) = $2(^{-}\Delta^{Ct})$. Primers used for real-time PCR are listed in Table S1.

ELISA

Mouse serum was collected by centrifuging peripheral blood at 3,000 rpm for 15 min a 4°C. For preparing tumor homogenates, 100 mg tumor tissue was homogenized with 1 mL chilled PBS and then centrifuged at 12,000 rpm for 10 min at 4°C to collect supernatant for ELISA.

Serum and tumor homogenates from LLC-bearing mice and supernatants from cultured NK cells were measured for TGF-β1 (R&D Systems, MN, USA), IFN-γ (R&D Systems, MN, USA), and GB (eBioscience, CA, USA) levels by ELISA.

Cytotoxicity Assay

LLC cells were harvested as target cells, and bone marrow-derived NK cells treated with AA or NG for 24 hr were harvested as effector cells. Cells were thoroughly washed and seeded in 96-well plates at the effector:target (E:T) ratios of 5:1, 10:1, and 20:1. They were incubated in a 5% CO_2 incubator at 37°C for 6 hr, and then we detected the LDH release of each well with CytoTox 96 Non-Radioactive Cytotoxicity Assay kit (Promega, WI, USA). Read absorbance was at 490 nm, and we calculated the percentage of NK cell-mediated cytotoxicity with the following formula.

$$\text{cytotoxicity} = \frac{\text{experimental} - \text{effector spontaneous} - \text{target spontaneous}}{\text{target maximum} - \text{target spontaneous}}$$

siRNA Transfection

Id2 and IRF2 were knocked down on freshly isolated mouse bone marrow cells, via transfecting small interfering RNA (siRNA) specific for IRF2 (5′-GCAAGCAGUACCUCAGCAATT-3′), siRNA specific for Id2 (5′-GCACGTCATCGATTACATC-3′), and nonsense control (5′-UUCUCCGAACGUGUCACGUTT-3′), respectively, on day 0 and day 4 with Lipofectamine RNAiMAX transfection system (Life Technologies, NY, USA) and Opti-MEM medium (Gibco, Thermo Fisher Scientific, MA, USA). Cells were collected on day 9 for flow cytometry analysis.

ChIP Assay

Bone marrow-derived NK cells were stimulated with 5 ng/mL TGF-β1 for 1 hr and collected by centrifuging at 3,000 rpm for 5 min. After fixing by cross-linking with 37% formaldehyde, total chromatin was isolated with SimpleChIP Enzymatic Chromatin IP Kit (Cell Signaling Technology, MA, USA). Cross-linked Smad3-DNA complexes were precipitated with Smad3 (C67H9) antibody (Cell Signaling Technology, MA, USA) and normal anti-rabbit immunoglobulin G (IgG) (Cell Signaling Technology, MA, USA). Targeted genomic regions were subsequently detected by PCR with specific primers for the predicted conserved Smad-binding site listed in Table S2 and analyzed with gel electrophoresis.

Statistical Analyses

Data are presented as mean ± SEM. All data were analyzed with GraphPad Prism 6.0 software (San Diego, CA, USA) by one-way ANOVA for single-variable analysis or two-way ANOVA for two independent variables analysis, followed by Tukey's multiple comparisons test.

SUPPLEMENTAL INFORMATION

Supplemental Information includes eleven figures and two tables and can be found with this article online at https://doi.org/10.1016/j.ymthe.2018.06.016.

AUTHOR CONTRIBUTIONS

Q.-M.W. and G.-Y.L. contributed equally to this work. G.-Y.L., Q.-M.W., P.M.-K.T., and S.Z. performed experiments, analyzed data, and contributed to manuscript preparation. X.-R.H. participated in animal experiments and contributed to data analysis. H.-Y.L. designed and supervised the entire study and revised the manuscript.

CONFLICTS OF INTEREST

The authors declare no conflict of interest.

ACKNOWLEDGMENTS

This study was supported by the Research Grants Council of Hong Kong (GRF 468513), the Innovation and Technology Fund of Hong Kong (ITS/227/15 and ITS/138/17), the Innovation and Technology Fund Internship Programme of Hong Kong (ITS-InP/242/16 and ITS-InP/347/17), the Hong Kong Scholar Program, and a direct grant for research from The Chinese University of Hong Kong (CUHK2016.035).

REFERENCES

1. Joyce, J.A. (2005). Therapeutic targeting of the tumor microenvironment. Cancer Cell *7*, 513–520.
2. Joyce, J.A., and Fearon, D.T. (2015). T cell exclusion, immune privilege, and the tumor microenvironment. Science *348*, 74–80.
3. Massagué, J. (2008). TGFbeta in Cancer. Cell *134*, 215–230.
4. Jakowlew, S.B. (2006). Transforming growth factor-beta in cancer and metastasis. Cancer Metastasis Rev. *25*, 435–457.
5. Yang, L., Pang, Y., and Moses, H.L. (2010). TGF-β and immune cells: an important regulatory axis in the tumor microenvironment and progression. Trends Immunol. *31*, 220–227.
6. Heldin, C.-H., Miyazono, K., and ten Dijke, P. (1997). TGF-beta signalling from cell membrane to nucleus through SMAD proteins. Nature *390*, 465–471.
7. Díaz-Valdés, N., Basagoiti, M., Dotor, J., Aranda, F., Monreal, I., Riezu-Boj, J.I., Borrás-Cuesta, F., Sarobe, P., and Feijoó, E. (2011). Induction of monocyte chemoattractant protein-1 and interleukin-10 by TGFbeta1 in melanoma enhances tumor infiltration and immunosuppression. Cancer Res. *71*, 812–821.
8. Li, A.G., Lu, S.-L., Zhang, M.-X., Deng, C., and Wang, X.-J. (2004). Smad3 knockout mice exhibit a resistance to skin chemical carcinogenesis. Cancer Res. *64*, 7836–7845.
9. Fan, Q., Gu, D., Liu, H., Yang, L., Zhang, X., Yoder, M.C., Kaplan, M.H., and Xie, J. (2014). Defective TGF-β signaling in bone marrow-derived cells prevents hedgehog-induced skin tumors. Cancer Res. *74*, 471–483.
10. Tang, P.M.-K., Zhou, S., Meng, X.-M., Wang, Q.-M., Li, C.-J., Lian, G.-Y., Huang, X.R., Tang, Y.J., Guan, X.Y., Yan, B.P., et al. (2017). Smad3 promotes cancer progression by inhibiting E4BP4-mediated NK cell development. Nat. Commun. *8*, 14677.
11. Derynck, R., and Zhang, Y.E. (2003). Smad-dependent and Smad-independent pathways in TGF-β family signalling. Nature *425*, 577–584.
12. Schmierer, B., and Hill, C.S. (2007). TGFbeta-SMAD signal transduction: molecular specificity and functional flexibility. Nat. Rev. Mol. Cell Biol. *8*, 970–982.
13. Zhang, S., Fei, T., Zhang, L., Zhang, R., Chen, F., Ning, Y., Han, Y., Feng, X.H., Meng, A., and Chen, Y.G. (2007). Smad7 antagonizes transforming growth factor β signaling in the nucleus by interfering with functional Smad-DNA complex formation. Mol. Cell. Biol. *27*, 4488–4499.
14. Wang, P., Fan, J., Chen, Z., Meng, Z.-Q., Luo, J.-M., Lin, J.-H., Zhou, Z.H., Chen, H., Wang, K., Xu, Z.D., and Liu, L.M. (2009). Low-level expression of Smad7 correlates with lymph node metastasis and poor prognosis in patients with pancreatic cancer. Ann. Surg. Oncol. *16*, 826–835.
15. Lamora, A., Talbot, J., Bougras, G., Amiaud, J., Leduc, M., Chesneau, J., Taurelle, J., Stresing, V., Le Deley, M.C., Heymann, M.F., et al. (2014). Overexpression of smad7 blocks primary tumor growth and lung metastasis development in osteosarcoma. Clin. Cancer Res. *20*, 5097–5112.
16. Feng, T., Dzieran, J., Gu, X., Marhenke, S., Vogel, A., Machida, K., Weiss, T.S., Ruemmele, P., Kollmar, O., Hoffmann, P., et al. (2015). Smad7 regulates compensatory hepatocyte proliferation in damaged mouse liver and positively relates to better clinical outcome in human hepatocellular carcinoma. Clin. Sci. (Lond.) *128*, 761–774.
17. Javelaud, D., Mohammad, K.S., McKenna, C.R., Fournier, P., Luciani, F., Niewolna, M., André, J., Delmas, V., Larue, L., Guise, T.A., and Mauviel, A. (2007). Stable overexpression of Smad7 in human melanoma cells impairs bone metastasis. Cancer Res. *67*, 2317–2324.
18. Javelaud, D., Delmas, V., Möller, M., Sextius, P., André, J., Menashi, S., Larue, L., and Mauviel, A. (2005). Stable overexpression of Smad7 in human melanoma cells inhibits their tumorigenicity in vitro and in vivo. Oncogene *24*, 7624–7629.
19. Teicher, B.A. (2001). Malignant cells, directors of the malignant process: role of transforming growth factor-beta. Cancer Metastasis Rev. *20*, 133–143.
20. Ghiringhelli, F., Puig, P.E., Roux, S., Parcellier, A., Schmitt, E., Solary, E., Kroemer, G., Martin, F., Chauffert, B., and Zitvogel, L. (2005). Tumor cells convert immature myeloid dendritic cells into TGF-β-secreting cells inducing CD4+CD25+ regulatory T cell proliferation. J. Exp. Med. *202*, 919–929.
21. Vivier, E., Raulet, D.H., Moretta, A., Caligiuri, M.A., Zitvogel, L., Lanier, L.L., Yokoyama, W.M., and Ugolini, S. (2011). Innate or adaptive immunity? The example of natural killer cells. Science *331*, 44–49.
22. Wakil, A.E., Wang, Z.E., Ryan, J.C., Fowell, D.J., and Locksley, R.M. (1998). Interferon gamma derived from CD4(+) T cells is sufficient to mediate T helper cell type 1 development. J. Exp. Med. *188*, 1651–1656.
23. Waldhauer, I., and Steinle, A. (2008). NK cells and cancer immunosurveillance. Oncogene *27*, 5932–5943.
24. Bellone, G., Aste-Amezaga, M., Trinchieri, G., and Rodeck, U. (1995). Regulation of NK cell functions by TGF-beta 1. J. Immunol. *155*, 1066–1073.
25. Ghiringhelli, F., Ménard, C., Terme, M., Flament, C., Taieb, J., Chaput, N., Puig, P.E., Novault, S., Escudier, B., Vivier, E., et al. (2005). CD4+CD25+ regulatory T cells inhibit natural killer cell functions in a transforming growth factor-β-dependent manner. J. Exp. Med. *202*, 1075–1085.
26. Flavell, R.A., Sanjabi, S., Wrzesinski, S.H., and Licona-Limón, P. (2010). The polarization of immune cells in the tumour environment by TGFbeta. Nat. Rev. Immunol. *10*, 554–567.
27. Marcoe, J.P., Lim, J.R., Schaubert, K.L., Fodil-Cornu, N., Matka, M., McCubbrey, A.L., Farr, A.R., Vidal, S.M., and Laouar, Y. (2012). TGF-β is responsible for NK cell immaturity during ontogeny and increased susceptibility to infection during mouse infancy. Nat. Immunol. *13*, 843–850.
28. Laouar, Y., Sutterwala, F.S., Gorelik, L., and Flavell, R.A. (2005). Transforming growth factor-beta controls T helper type 1 cell development through regulation of natural killer cell interferon-gamma. Nat. Immunol. *6*, 600–607.
29. Castriconi, R., Cantoni, C., Della Chiesa, M., Vitale, M., Marcenaro, E., Conte, R., Biassoni, R., Bottino, C., Moretta, L., and Moretta, A. (2003). Transforming growth

factor beta 1 inhibits expression of NKp30 and NKG2D receptors: consequences for the NK-mediated killing of dendritic cells. Proc. Natl. Acad. Sci. USA *100*, 4120–4125.

30. Lee, J.-C., Lee, K.-M., Kim, D.-W., and Heo, D.S. (2004). Elevated TGF-β1 secretion and down-modulation of NKG2D underlies impaired NK cytotoxicity in cancer patients. J. Immunol. *172*, 7335–7340.
31. Trotta, R., Dal Col, J., Yu, J., Ciarlariello, D., Thomas, B., Zhang, X., Allard, J., 2nd, Wei, M., Mao, H., Byrd, J.C., et al. (2008). TGF-β utilizes SMAD3 to inhibit CD16-mediated IFN-γ production and antibody-dependent cellular cytotoxicity in human NK cells. J. Immunol. *181*, 3784–3792.
32. Tang, L.X., He, R.H., Yang, G., Tan, J.J., Zhou, L., Meng, X.M., Huang, X.R., and Lan, H.Y. (2012). Asiatic acid inhibits liver fibrosis by blocking TGF-beta/Smad signaling in vivo and in vitro. PLoS ONE *7*, e31350.
33. Liu, X., Wang, W., Hu, H., Tang, N., Zhang, C., Liang, W., and Wang, M. (2006). Smad3 specific inhibitor, naringenin, decreases the expression of extracellular matrix induced by TGF-β1 in cultured rat hepatic stellate cells. Pharm. Res. *23*, 82–89.
34. Du, G., Jin, L., Han, X., Song, Z., Zhang, H., and Liang, W. (2009). Naringenin: a potential immunomodulator for inhibiting lung fibrosis and metastasis. Cancer Res. *69*, 3205–3212.
35. Meng, X.M., Zhang, Y., Huang, X.-R., Ren, G.L., Li, J., and Lan, H.Y. (2015). Treatment of renal fibrosis by rebalancing TGF-β/Smad signaling with the combination of asiatic acid and naringenin. Oncotarget *6*, 36984–36997.
36. Wendel, M., Galani, I.E., Suri-Payer, E., and Cerwenka, A. (2008). Natural killer cell accumulation in tumors is dependent on IFN-gamma and CXCR3 ligands. Cancer Res. *68*, 8437–8445.
37. Marçais, A., Viel, S., Grau, M., Henry, T., Marvel, J., and Walzer, T. (2013). Regulation of mouse NK cell development and function by cytokines. Front. Immunol. *4*, 450.
38. Di Santo, J.P. (2006). Natural killer cell developmental pathways: a question of balance. Annu. Rev. Immunol. *24*, 257–286.
39. Ikawa, T., Fujimoto, S., Kawamoto, H., Katsura, Y., and Yokota, Y. (2001). Commitment to natural killer cells requires the helix-loop-helix inhibitor Id2. Proc. Natl. Acad. Sci. USA *98*, 5164–5169.
40. Taki, S., Nakajima, S., Ichikawa, E., Saito, T., and Hida, S. (2005). IFN regulatory factor-2 deficiency revealed a novel checkpoint critical for the generation of peripheral NK cells. J. Immunol. *174*, 6005–6012.
41. Loots, G., and Ovcharenko, I. (2007). ECRbase: database of evolutionary conserved regions, promoters, and transcription factor binding sites in vertebrate genomes. Bioinformatics *23*, 122–124.
42. Kopp, H.-G., Placke, T., and Salih, H.R. (2009). Platelet-derived transforming growth factor-β down-regulates NKG2D thereby inhibiting natural killer cell antitumor reactivity. Cancer Res. *69*, 7775–7783.
43. Boos, M.D., Yokota, Y., Eberl, G., and Kee, B.L. (2007). Mature natural killer cell and lymphoid tissue-inducing cell development requires Id2-mediated suppression of E protein activity. J. Exp. Med. *204*, 1119–1130.
44. Yokota, Y., Mansouri, A., Mori, S., Sugawara, S., Adachi, S., Nishikawa, S., and Gruss, P. (1999). Development of peripheral lymphoid organs and natural killer cells depends on the helix-loop-helix inhibitor Id2. Nature *397*, 702–706.
45. Lohoff, M., Duncan, G.S., Ferrick, D., Mittrücker, H.-W., Bischof, S., Prechtl, S., Röllinghoff, M., Schmitt, E., Pahl, A., and Mak, T.W. (2000). Deficiency in the transcription factor interferon regulatory factor (IRF)-2 leads to severely compromised development of natural killer and T helper type 1 cells. J. Exp. Med. *192*, 325–336.
46. Thomas, D.A., and Massagué, J. (2005). TGF-β directly targets cytotoxic T cell functions during tumor evasion of immune surveillance. Cancer Cell *8*, 369–380.
47. Yu, J., Wei, M., Becknell, B., Trotta, R., Liu, S., Boyd, Z., Jaung, M.S., Blaser, B.W., Sun, J., Benson, D.M., Jr., et al. (2006). Pro- and antiinflammatory cytokine signaling: reciprocal antagonism regulates interferon-gamma production by human natural killer cells. Immunity *24*, 575–590.
48. Budhu, S., Schaer, D.A., Li, Y., Toledo-Crow, R., Panageas, K., Yang, X., Zhong, H., Houghton, A.N., Silverstein, S.C., Merghoub, T., and Wolchok, J.D. (2017). Blockade of surface-bound TGF-β on regulatory T cells abrogates suppression of effector T cell function in the tumor microenvironment. Sci. Signal. *10*, eaak9702.
49. Mariathasan, S., Turley, S.J., Nickles, D., Castiglioni, A., Yuen, K., Wang, Y., Kadel, E.E., III, Koeppen, H., Astarita, J.L., Cubas, R., et al. (2018). TGFβ attenuates tumour response to PD-L1 blockade by contributing to exclusion of T cells. Nature *554*, 544–548.
50. Tauriello, D.V.F., Palomo-Ponce, S., Stork, D., Berenguer-Llergo, A., Badia-Ramentol, J., Iglesias, M., Sevillano, M., Ibiza, S., Cañellas, A., Hernando-Momblona, X., et al. (2018). TGFβ drives immune evasion in genetically reconstituted colon cancer metastasis. Nature *554*, 538–543.
51. Lee, Y.S., Jin, D.-Q., Kwon, E.J., Park, S.H., Lee, E.-S., Jeong, T.C., Nam, D.H., Huh, K., and Kim, J.A. (2002). Asiatic acid, a triterpene, induces apoptosis through intracellular Ca2+ release and enhanced expression of p53 in HepG2 human hepatoma cells. Cancer Lett. *186*, 83–91.
52. Hsu, Y.-L., Kuo, P.-L., Lin, L.-T., and Lin, C.-C. (2005). Asiatic acid, a triterpene, induces apoptosis and cell cycle arrest through activation of extracellular signal-regulated kinase and p38 mitogen-activated protein kinase pathways in human breast cancer cells. J. Pharmacol. Exp. Ther. *313*, 333–344.
53. Park, B.C., Bosire, K.O., Lee, E.-S., Lee, Y.S., and Kim, J.-A. (2005). Asiatic acid induces apoptosis in SK-MEL-2 human melanoma cells. Cancer Lett. *218*, 81–90.
54. Kavitha, C.V., Agarwal, C., Agarwal, R., and Deep, G. (2011). Asiatic acid inhibits pro-angiogenic effects of VEGF and human gliomas in endothelial cell culture models. PLoS ONE *6*, e22745.
55. Lou, C., Zhang, F., Yang, M., Zhao, J., Zeng, W., Fang, X., Zhang, Y., Zhang, C., and Liang, W. (2012). Naringenin decreases invasiveness and metastasis by inhibiting TGF-β-induced epithelial to mesenchymal transition in pancreatic cancer cells. PLoS ONE *7*, e50956.
56. Jin, C.Y., Park, C., Hwang, H.J., Kim, G.Y., Choi, B.T., Kim, W.J., and Choi, Y.H. (2011). Naringenin up-regulates the expression of death receptor 5 and enhances TRAIL-induced apoptosis in human lung cancer A549 cells. Mol. Nutr. Food Res. *55*, 300–309.
57. Hsiao, Y.-C., Hsieh, Y.-S., Kuo, W.-H., Chiou, H.-L., Yang, S.-F., Chiang, W.-L., and Chu, S.C. (2007). The tumor-growth inhibitory activity of flavanone and 2′-OH flavanone in vitro and in vivo through induction of cell cycle arrest and suppression of cyclins and CDKs. J. Biomed. Sci. *14*, 107–119.
58. Ishigame, H., Zenewicz, L.A., Sanjabi, S., Licona-Limón, P., Nakayama, M., Leonard, W.J., and Flavell, R.A. (2013). Excessive Th1 responses due to the absence of TGF-β signaling cause autoimmune diabetes and dysregulated Treg cell homeostasis. Proc. Natl. Acad. Sci. USA *110*, 6961–6966.
59. Vermeire, S. (2015). Oral SMAD7 antisense drug for Crohn's disease. N. Engl. J. Med. *372*, 1166–1167.

YMTHE, Volume *26*

Supplemental Information

Combination of Asiatic Acid and Naringenin Modulates NK Cell Anti-cancer Immunity by Rebalancing Smad3/Smad7 Signaling

Guang-Yu Lian, Qing-Ming Wang, Patrick Ming-Kuen Tang, Shuang Zhou, Xiao-Ru Huang, and Hui-Yao Lan

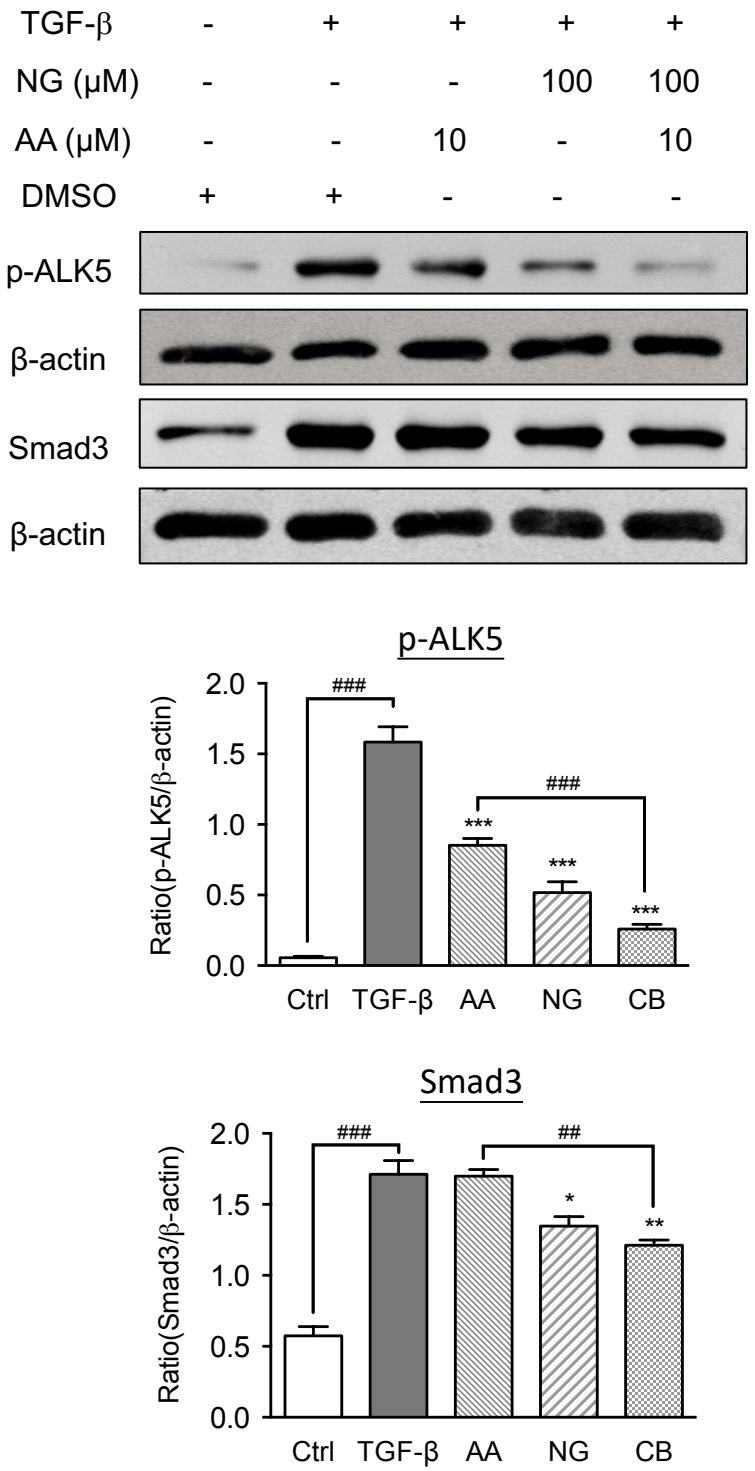

Figure S1. Combination of AA and NG produces a better suppressive effect on TGF-β1-induced p-ALK5 and Smad3 expression in bone marrow-derived NK (BM-NK) cells. NK cells were pre-incubated with AA, NG or their combination for overnight before being stimulated with TGF-β1 (5ng/ml) for p-ALK5 at 15 minutes or expression of Smad3 protein at 24 hours. Each bar represents the mean ± SEM for groups of three independent experiments. * $p<0.05$, ** $p<0.01$, *** $p<0.001$ compared to TGF-β; ## $p<0.05$, ### $p<0.001$ as indicated.

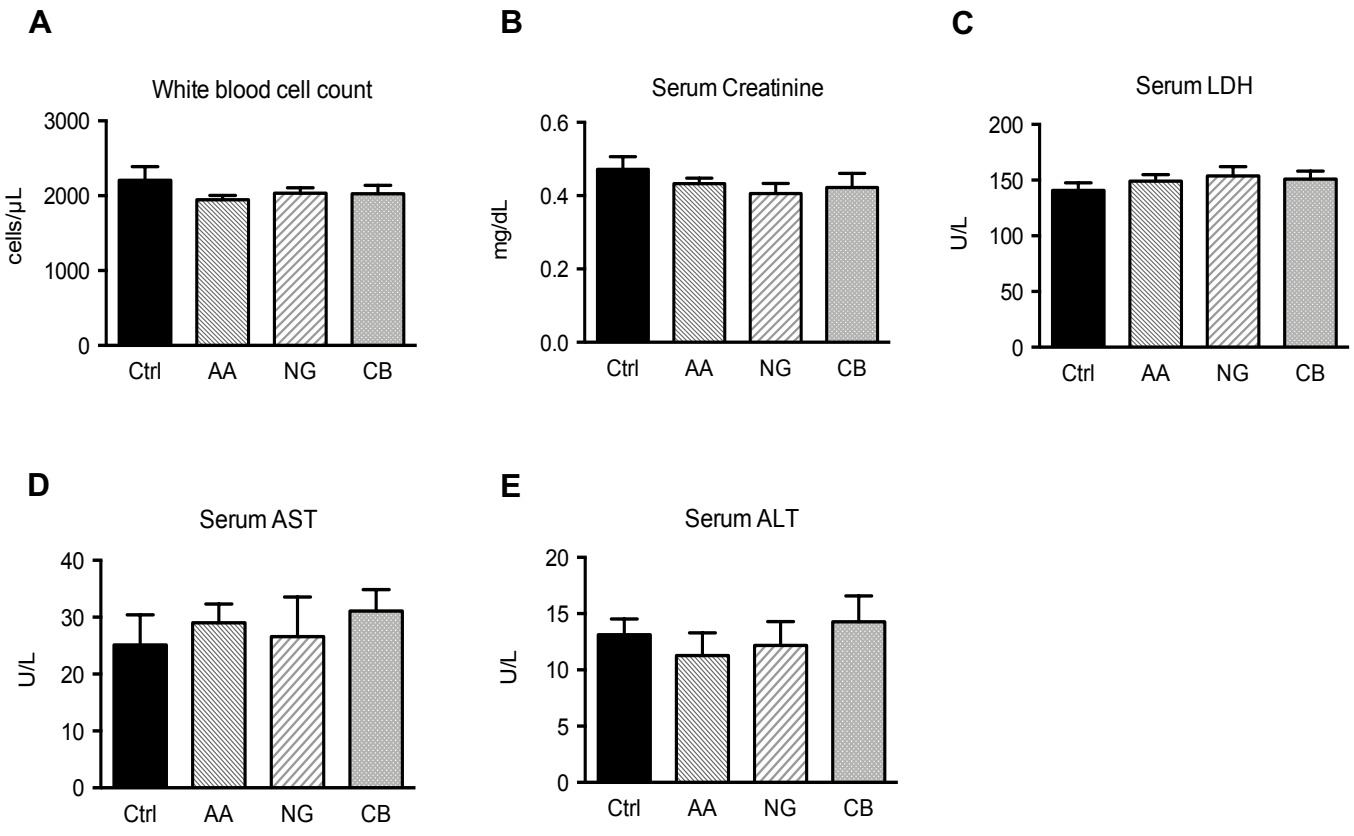

Figure S2. Treatment with AA, NG, or their combination does not induce side effects on LLC- bearing mice. (A) White blood cell counts, serum levels of **(B)** creatinine **(C)** LDH **(D)** AST and **(E)** ALT from LLC bearing mice at 27 days after tumor inoculation. Note that either individual or combination therapy with AA and NG does not cause toxicity to LLC-bearing mice. Each bar represents the mean ± SEM for groups of three to four mice.

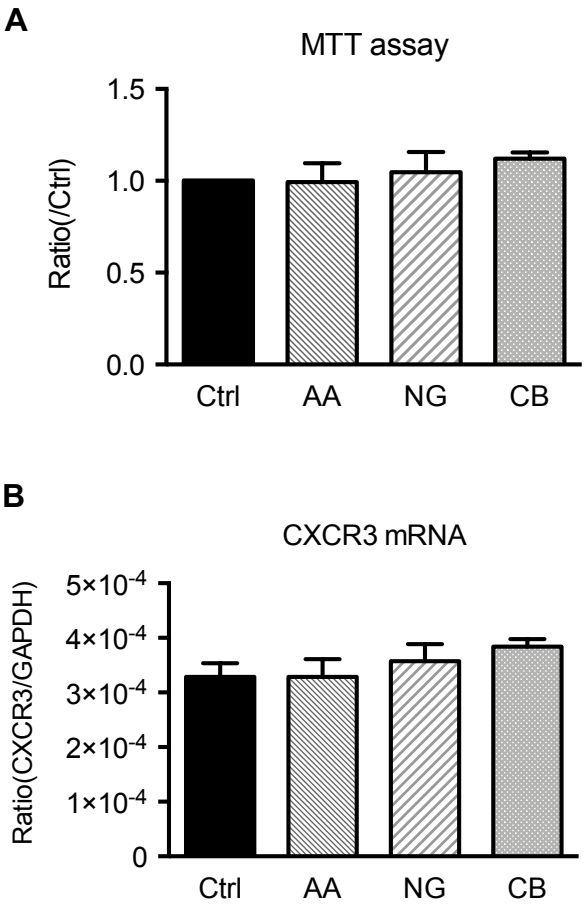

Figure S3. Treatment with AA, NG, or their combination does not influence NK cell proliferation and expression of CXCR3. (A) MTT assay shows that treatment with AA, NG or their combination does not alter BM-NK cell proliferation. **(B)** mRNA levels of CXCR3, a chemokine receptor critical for NK infiltration in tumor microenvironment detected by real-time PCR. Each bar represents the mean ± SEM for groups of three independent experiments.

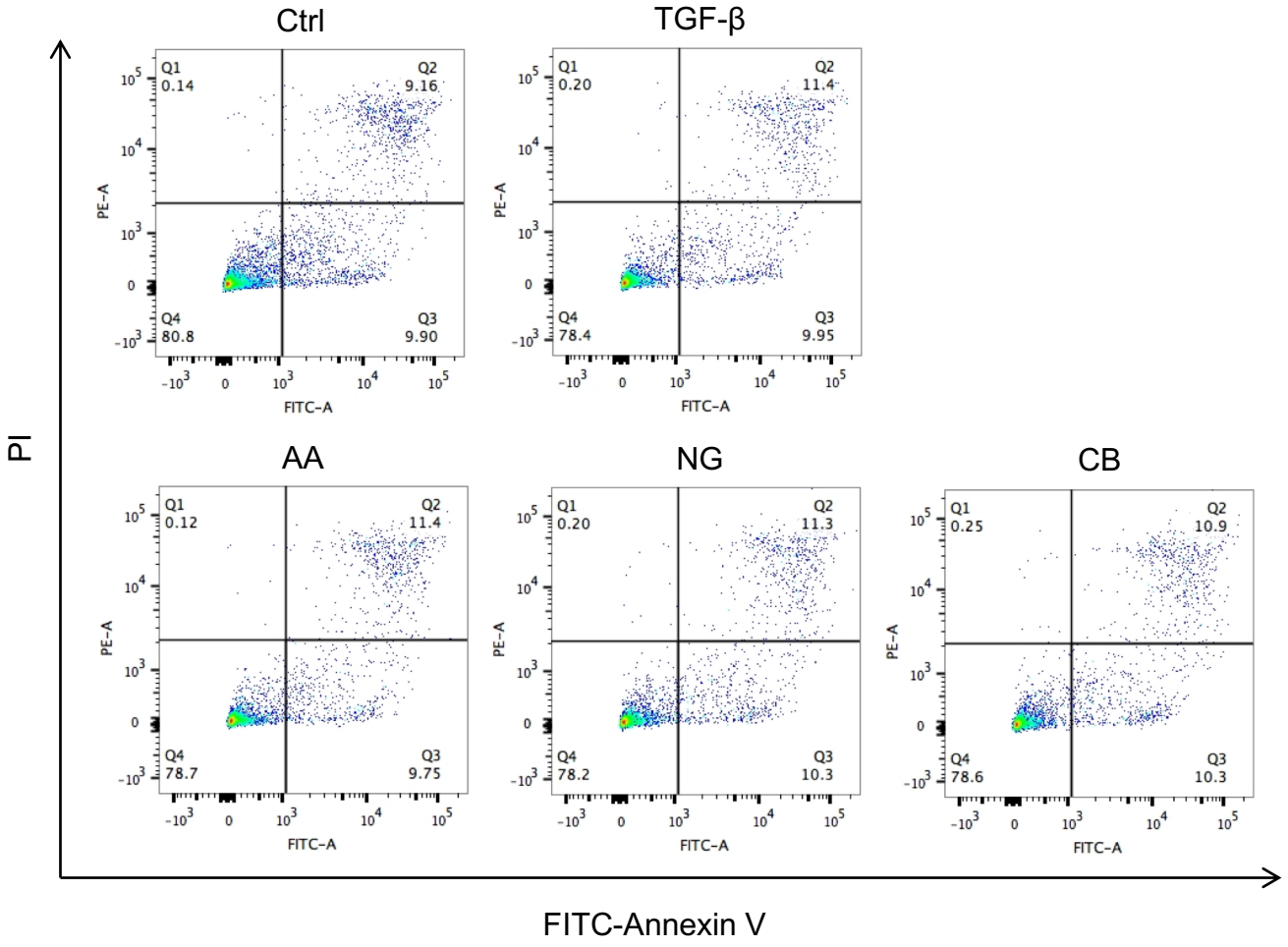

Figure S4. Neither individual nor combination therapy with AA and NG influences NK cell apoptosis. Individual or combination of AA and NG pre-treated BM-NK cells were stimulated with 5ng/ml TGF-β1 for 24 hours and then stained with FITC-Annexin V and PI to identify apoptotic NK cells. Results show that treatment with AA, NG or combination of AA and NG does not alter TGF-β1-induced NK cell apoptosis. Results represent three independent experiments.

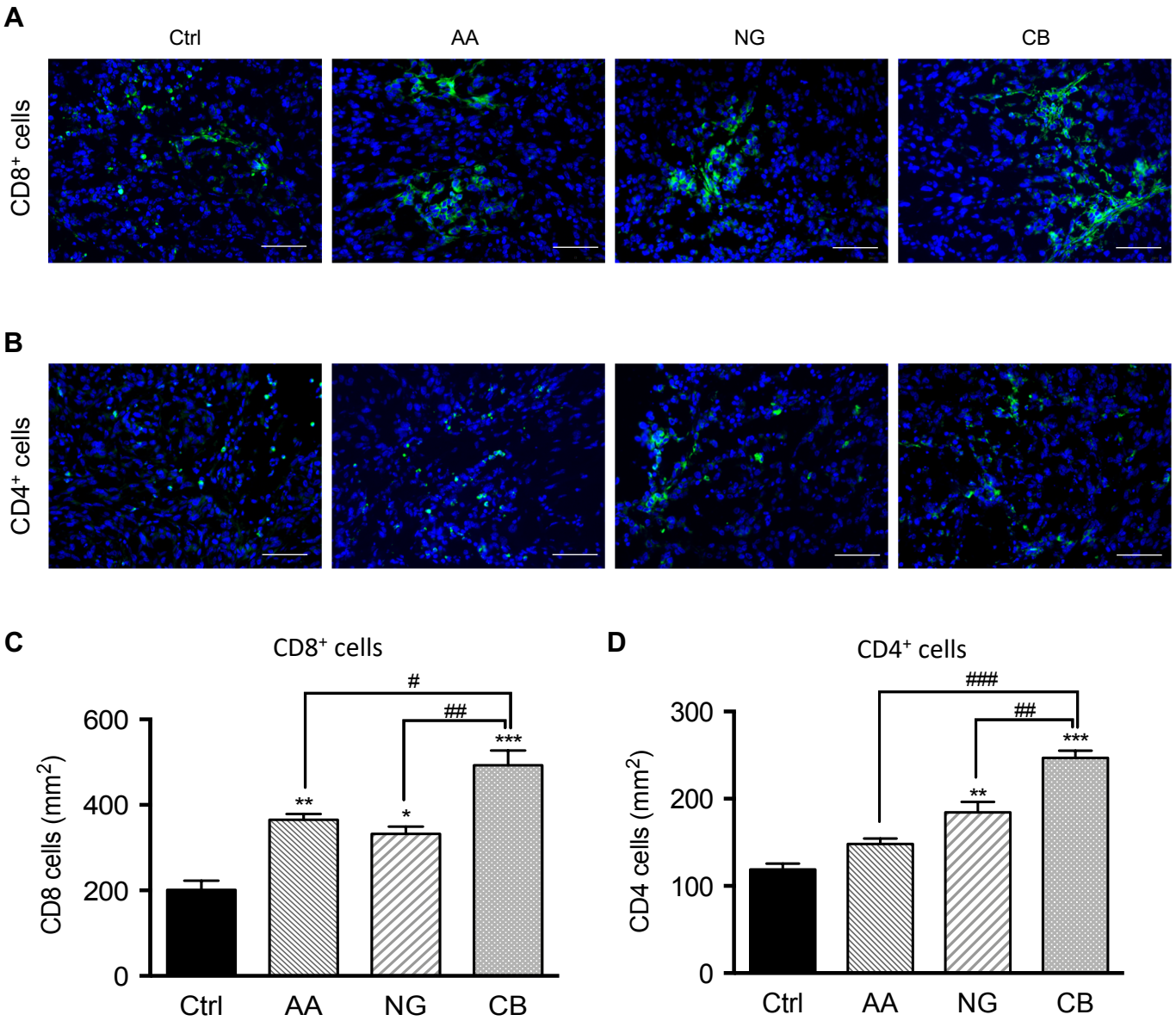

Figure S5. Combination therapy enhances the accumulation of CD8⁺ and CD4⁺ cells in tumor microenvironment. (A) Infiltrated CD8⁺ cells detected with FITC-CD8 and **(B**) infiltrated CD4⁺ cells detected with FITC-CD4 in LLC tumor microenvironment. Each bar represents the mean ± SEM for groups of three mice. * $p<0.05$, ** $p<0.01$, *** $p<0.001$ compared to Ctrl; # $p<0.05$, ## $p<0.01$, ### $p<0.001$ as indicated. Scale bar, 100µm.

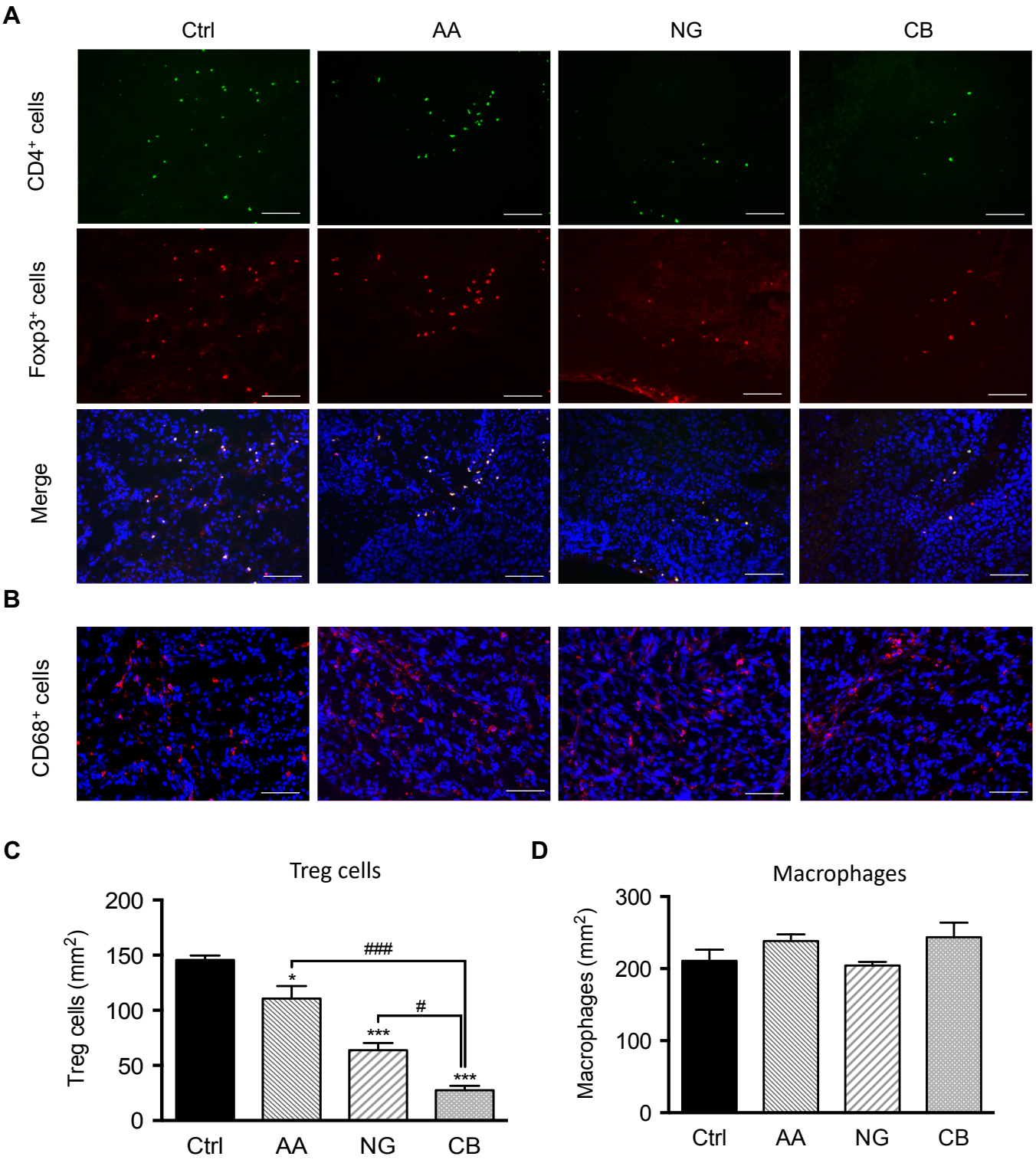

Figure S6. Combination therapy inhibits the accumulation of regulatory T cells (Tregs) while does not influence the accumulation of macrophages in tumor microenvironment. (A) Infiltrated Tregs were detected with FITC-CD4 and PE-Foxp3 and **(B)** infiltrated Tregs were detected with PE-CD68 in LLC tumor microenvironment. Each bar represents the mean ± SEM for groups of three mice. * $p<0.05$, *** $p<0.001$ compared to Ctrl; # $p<0.05$, ### $p<0.001$ as indicated. Scale bar, 100μm.

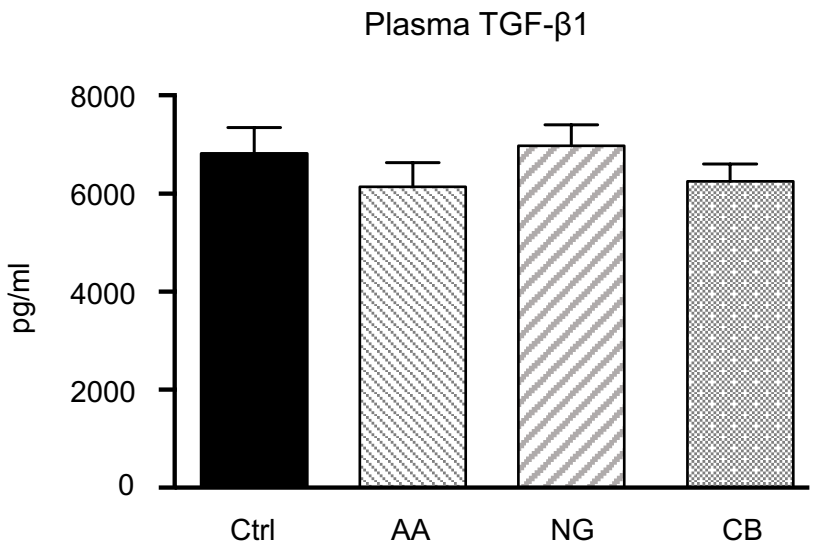

Figure S7. Combination therapy does not influence plasma levels of TGF-β1 in LLC-bearing mice. Each bar represents the mean ± SEM for groups of four to five mice.

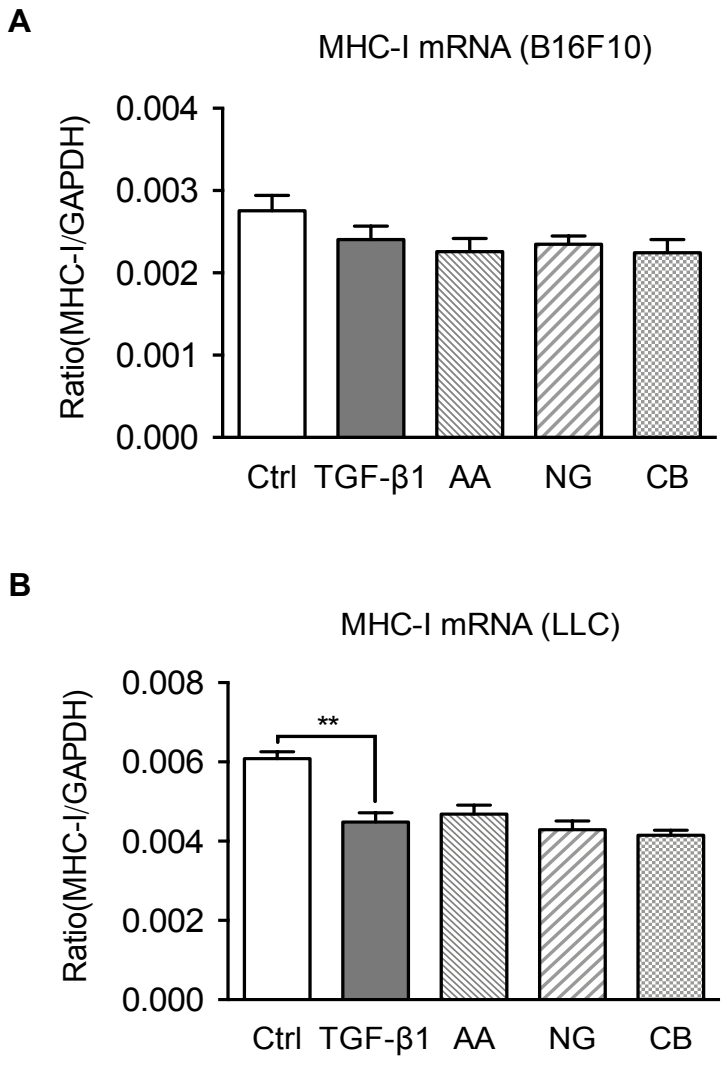

Figure S8. Treatment with AA, NG or their combination does not influence TGF-β1-induced inhibition on MHC-I expression on B16F10 and LLC cells. mRNA levels of MHC-I in **(A)** B16F10 and **(B)** LLC cells. Note that pre-treatment with AA, NG or their combination (CB) does not influence MHC-I expression in response to TGF-β1 (5ng/ml) stimulation in both B16F10 melanoma and LLC lung carcinoma cells. Each bar represents the mean ± SEM for groups of three independent experiments. ** $p<0.01$ compared to TGF-β1.

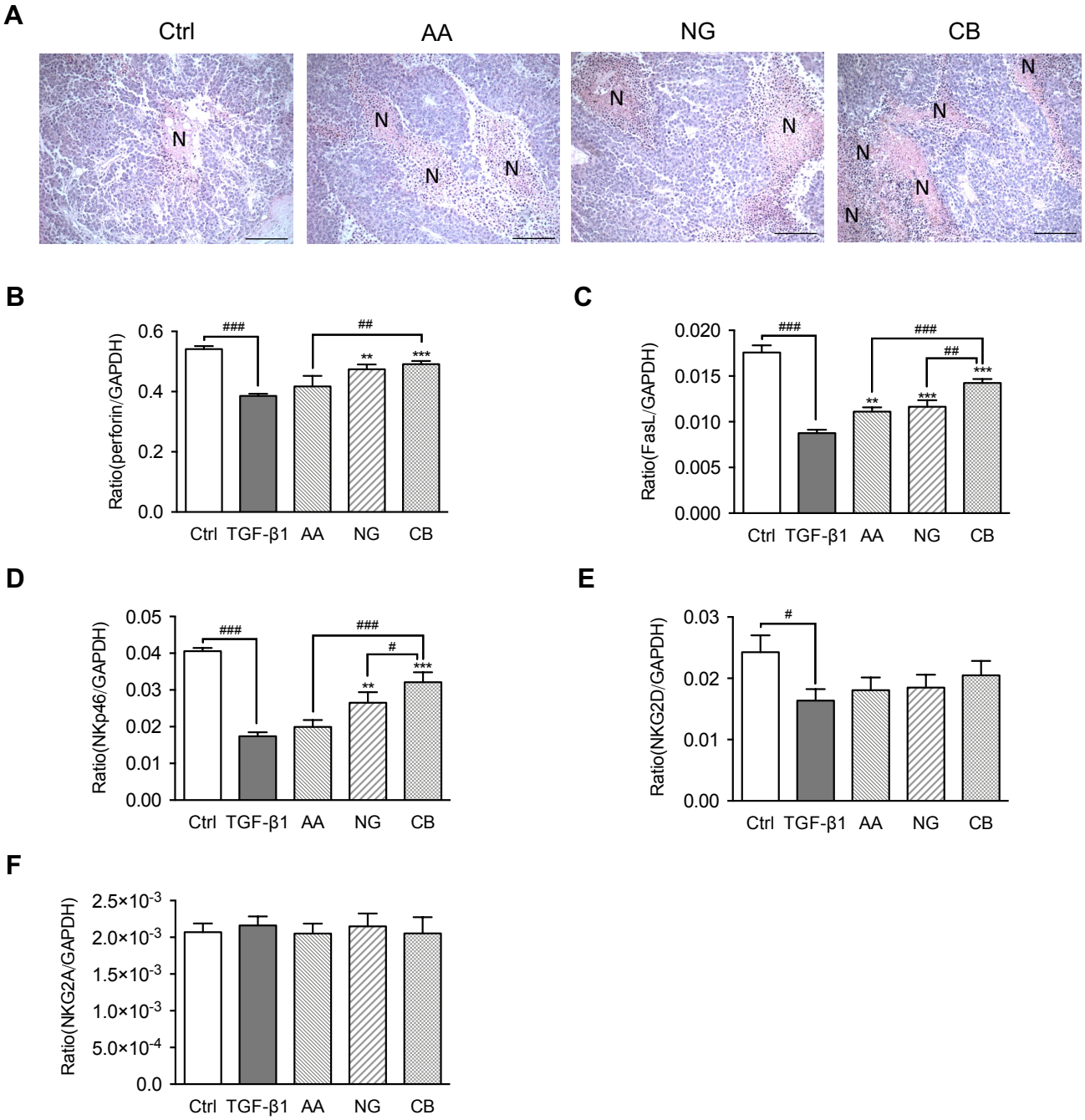

Figure S9. Combination therapy promotes NK-mediated anti-cancer activity via enhancing the expression of cytotoxic mediators and activation receptors in NK cells. (A) Periodic acid–Schiff (PAS) staining shows an increment of intratumoral necrosis (N indicated) in melanoma induced by combination therapy compared with control. mRNA levels of **(B)** perforin, **(C)** Fas ligand (FasL), **(D)** NKp46, **(E)** NKG2D and **(F)** NKG2A in splenic NK cells with TGF-β1 stimulation were detected by real-time PCR. Note that the combination treatment with AA and NG increases tumor necrosis in melanoma and produces a better anti-tumor effect compared to monotherapy by promoting NK cell activation (NKp46) and cytotoxicity (perforin, Fas ligand) in response to TGF-β1, although no alteration is found on expression of NKG2A and NKG2D expression. Each bar represents the mean ± SEM for groups of three independent experiments. ** $p<0.01$, *** $p<0.001$ compared to TGF-β1; # $p<0.05$, ## $p<0.01$, ### $p<0.001$ as indicated. Scale bar, 200μm.

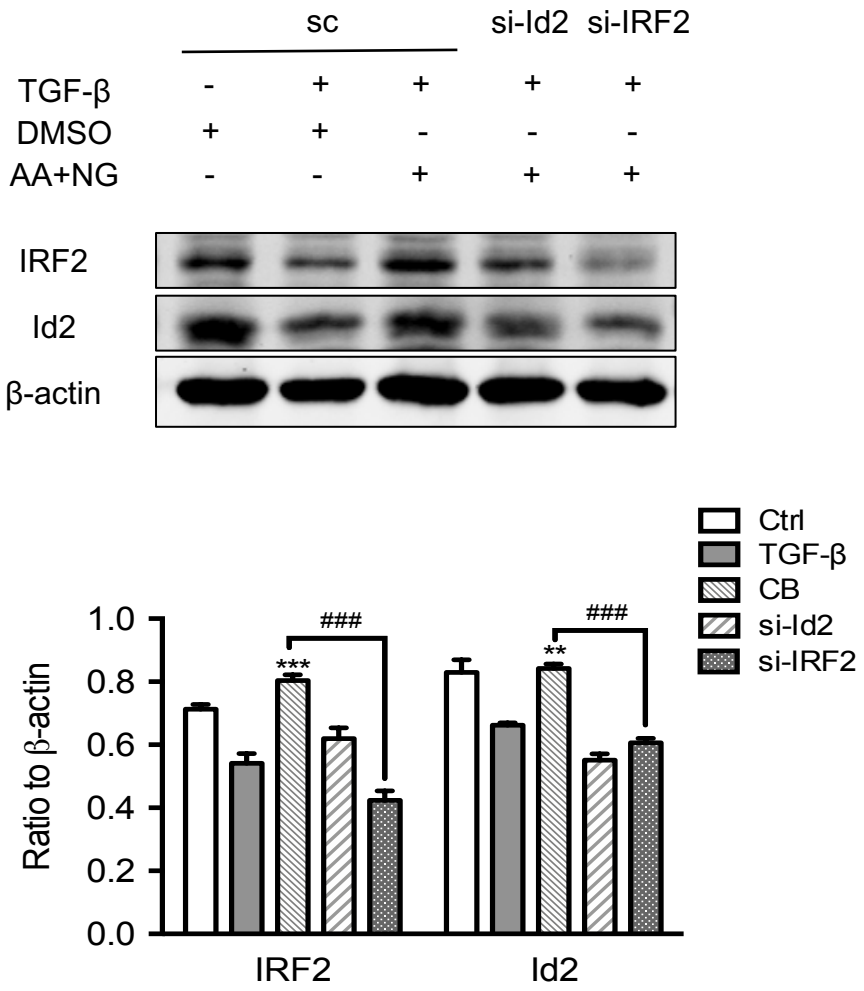

Figure S10. Knocking down Id2 and IRF2 prevents the counter-regulatory effect of AA and NG on TGF-β1-induced suppression of IRF2 and Id2 expression in BM-NK cells. BM-NK cells were transfected with scramble sequence (sc), si-Id2 or si-IRF2 and then cultured with AA (10μM) and NG (100μM) under TGF-β1 (5ng/ml) conditions for 9 days. Each bar represents the mean ± SEM for groups of three independent experiments. ** p<0.01, *** p<0.001 compared to TGF-β1; ### p<0.001 as indicated.

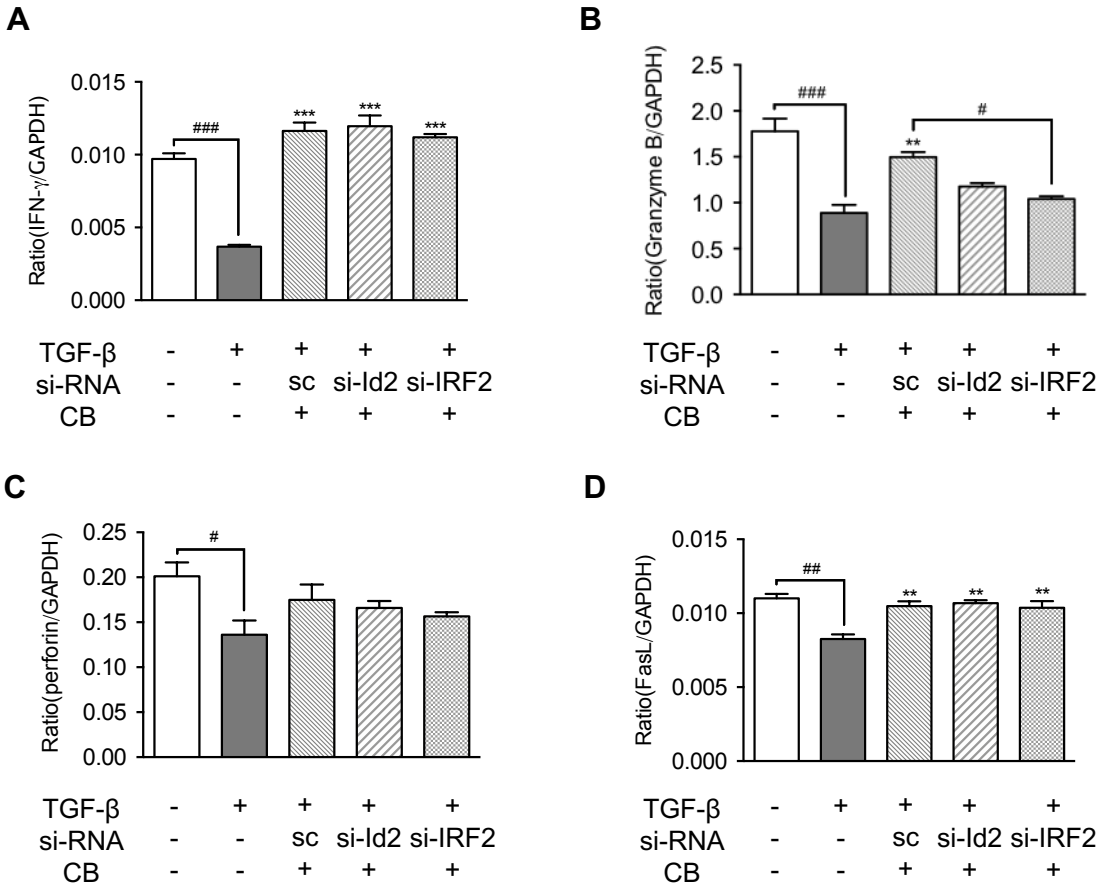

Figure S11. Expression of cytotoxic mediators in BM-NK cells treated with specific siRNA sequence for Id2 and IRF2. mRNA levels of **(A)** IFN-γ, **(B)** granzyme B, **(C)** perforin, **(D)** Fas ligand (FasL) in mature BM-NK cells transfected with scramble sequence (sc), si-Id2 or si-IRF2 with TGF-β1 (5ng/ml) stimulation. Each bar represents the mean ± SEM for groups of three independent experiments. ** $p<0.01$, *** $p<0.001$ compared to TGF-β1; # $p<0.05$, ## $p<0.01$, ### $p<0.001$ as indicated.

Table S1. Sequence of primers for real-time PCR

Primers for Real-time PCR		
Target Gene	Forward Primer	Reverse Primer
Id2	ACCAGAGACCTGGACAGAAC	AAGCTCAGAAGGGAATTCAG
IRF2	CTTATCCGAACGACCTTCCA	CTTGCTGTCCAGATGGGACT
CXCR3	TGCTAGATGCCTCGGACTTT	CGCTGACTCAGTAGCACAATT
MHC-I	GAGGGTGGCTCTCACACATTC	TTGGCCTTCGTAAGCAAACTG
IFN-γ	TTTCGCCTTGCTGTTGCTGA	TGGATATCTGGAGGAACTGGCA
granzyme B	TGCTGCTAAAGCTGAAGAGTAAG	CGTGTTTGAGTATTTGCCCATTG
perforin	GCTCCCACTCCAAGGTAGC	GCTCCCACTCCAAGGTAGC
FasL	GCCCATGAATTACCCATGTCC	ACAGATTTGTGTTGTGGTCCTT
NKp46	ATGCTGCCAACACTCACTG	GATGTTCACCGAGTTTCCATTTG
NKG2D	ACTCAGAGATGAGCAAATGCC	CAGGTTGACTGGTAGTTAGTGC
NKG2A	GCCCCTGCAAAGATACCGAA	TCTGTGGGTTCTAGTCATTGAGG
GAPDH	GCATGGCCTTCCGTGTTC	GATGTCATCATACTTGGCAGGTTT

Table S2. Sequence of primers for ChIP assay

Primers for ChIP Assay		
Target Gene	Forward Primer	Reverse Primer
Id2 SBS1	GGGGTGAGAGAACAGAAGGA	TTTCAGACAACCAGTGCTTTG
Id2 SBS2	CAGCATTCAGTAGGCTCGTG	GCCTTTTCACAAAGGTGGAG
IRF2 5'UTR SBS1	GGTGTCGTGTGTTGTGGGTA	GGTGGCGACAGTGTCTGTAA
IRF2 3'UTR SBS2	GTGTCTCAGCTCCACCCATT	CTCCTATGCTCAGCCTGTCC